Communications Medicine

https://doi.org/10.1038/s43856-026-01744-x

Article in Press

Enhancement of sleep slow wave activity using transcranial electrical stimulation with temporal interference: an interim analysis of the STRENGTHEN study

Received: 5 August 2025

Accepted: 15 June 2026

Published online: 01 July 2026

Cite this article as: Schaeffer, E.L., Haber, I., Fan, Z. *et al.* Enhancement of sleep slow wave activity using transcranial electrical stimulation with temporal interference: an interim analysis of the STRENGTHEN study. *Commun Med* (2026). https://doi.org/10.1038/s43856-026-01744-x

Erin L. Schaeffer, Ido Haber, Zhiwei Fan, Simone Bruno, Beril Mat, Tariq Alauddin, Giulietta Vigueras, Lindsey Neumann, Richard Smith, Florian Missey, Adam Williamson, Peter Achermann, Stefan Beerli, Myles Capstick, Esra Neufeld, Niels Kuster, Robin I. Goldman, Richard J. Davidson, William Marshall, Larissa Albantakis, Stephanie G. Jones, Chiara Cirelli, Melanie Boly & Giulio Tononi

ARTICLE IN PRESS

We are providing an unedited version of this manuscript to give early access to its findings. Before final publication, the manuscript will undergo further editing. Please note there may be errors present which affect the content, and all legal disclaimers apply.

If this paper is publishing under a Transparent Peer Review model then Peer Review reports will publish with the final article.

© The Author(s) 2026. **Open Access** This article is licensed under a Creative Commons Attribution 4.0 International License, which permits use, sharing, adaptation, distribution and reproduction in any medium or format, as long as you give appropriate credit to the original author(s) and the source, provide a link to the Creative Commons licence, and indicate if changes were made. The images or other third party material in this article are included in the article's Creative Commons licence, unless indicated otherwise in a credit line to the material. If material is not included in the article's Creative Commons licence and your intended use is not permitted by statutory regulation or exceeds the permitted use, you will need to obtain permission directly from the copyright holder. To view a copy of this licence, visit http://creativecommons.org/licenses/by/4.0/.

ARTICLE IN PRESS

Enhancement of Sleep Slow Wave Activity using Transcranial Electrical Stimulation with Temporal Interference: An Interim Analysis of the STRENGTHEN Study

Erin L. Schaeffer[1,2], Ido Haber[1,3], Zhiwei Fan[1,4], Simone Bruno[1], Beril Mat[1], Tariq Alauddin[1], Giulietta Vigueras[1], Lindsey Neumann[1], Richard Smith[1], Florian Missey[5,6], Adam Williamson[5,6], Peter Achermann[7,8], Stefan Beerli[8], Myles Capstick[8], Esra Neufeld[8], Niels Kuster[8,9], Robin I. Goldman[10], Richard J. Davidson[10,11], William Marshall[1,12], Larissa Albantakis[1], Stephanie G. Jones[1], Chiara Cirelli[1#], Melanie Boly[13#]*, Giulio Tononi[1#]*

Affiliations

1. Department of Psychiatry, University of Wisconsin-Madison, Madison, Wisconsin
2. Medical Scientist Training Program, University of Wisconsin-Madison, Madison, Wisconsin
3. Department of Biomedical Engineering, University of Wisconsin-Madison, Madison, Wisconsin
4. International Institute for Integrative Sleep Medicine (WPI-IIIS), Tsukuba Institute for Advanced Research (TIAR), University of Tsukuba, Tsukuba, Japan
5. International Clinical Research Center, St. Anne's University Hospital Brno, Brno, Czech Republic
6. Institute de Neurosciences des Systèmes (INS), INSERM, Aix-Marseille Université, Marseille, France
7. Institute of Pharmacology and Toxicology, University of Zurich, Zurich, Switzerland
8. Foundation for Research on Information Technologies in Society (IT'IS), Zurich, Switzerland
9. Department of Information Technology and Electrical Engineering, Swiss Federal Institute of Technology (ETH) Zurich, Zurich, Switzerland
10. Center for Healthy Minds, University of Wisconsin-Madison, Madison, Wisconsin
11. Department of Psychology, University of Wisconsin-Madison, Madison, Wisconsin
12. Department of Mathematics and Statistics, Brock University, St. Catharines, Ontario, Canada
13. Department of Neurology, University of Wisconsin-Madison, Madison, Wisconsin

Senior authors: Chiara Cirelli, Melanie Boly and Giulio Tononi
*Corresponding authors:

Giulio Tononi
Dept. of Psychiatry
University of Wisconsin-Madison
6001 Research Park Blvd
Madison, WI 53719, USA
gtononi@wisc.edu

Melanie Boly
Dept. of Neurology
University of Wisconsin-Madison
600 Highland Ave
Madison, WI 53792, USA
boly@neurology.wisc.edu

ARTICLE IN PRESS

Abstract

Background: Slow waves are oscillations that reflect rhythmic alternation of neuronal activity and mediate key restorative functions of non-rapid eye movement (NREM) sleep. Left ventromedial prefrontal cortex regions are a "hot spot" for slow wave generation. The enhancement of slow wave activity (SWA, 0.5-4 Hz) has been shown to be beneficial, as in improving memory performance. To overcome limitations of current techniques, we assessed the ability of a non-invasive neuromodulatory tool, Transcranial Electrical Stimulation with Temporal Interference (TES-TI), to enhance SWA during NREM sleep overnight in healthy humans.

Methods: The current study is an interim analysis focused on the effects of TES-TI during NREM sleep in a laboratory setting. Two high frequency carriers with 1Hz difference (TES^{15kHz}-TI^{1Hz}) produced amplitude-modulated temporal interference at 1Hz. Data were collected at the University of Wisconsin-Madison as part of the ongoing STRENGTHEN study (ClinicalTrials.gov, NCT06267521, 02/12/2024, single-blind, non-random allocation). Eligible participants were healthy adults (ages 18–50) assigned in parallel to one of four groups: (Group 1) TES^{15kHz} (0 Hz difference frequency) 2 nights per week and meditation; (Group 2) TES^{15kHz}-TI^{1Hz} (1 Hz difference frequency) 2 nights per week and sham meditation; (Group 3) TES^{15kHz}-TI^{1Hz} 1 night per week and meditation; (Group 4) TES^{15kHz}-TI^{1Hz} 2 nights per week and meditation. Stimulation targeting left ventromedial prefrontal cortex occurred during NREM sleep over repeated nights (~10 stimulation periods, 3-min each, first half of night, 1-2 nights/week, 4-week protocol). Twenty-one participants (Groups 2, 3, 4) received TES^{15kHz}-TI^{1Hz} and seven participants received TES^{15kHz} (Group 1). SWA was measured using simultaneous high-density electroencephalography with polysomnography.

Results: We show that SWA is increased with TES^{15kHz}-TI^{1Hz} (N = 21 total; N = 5 Group 2, N = 10 Group 3, N = 6 Group 4), and the effect outlasts the stimulation period; higher frequencies (sigma and beta) decrease. During stimulation, SWA is greater in TES^{15kHz}-TI^{1Hz} than pure TES^{15kHz} (N = 7 Group 1). The incremental effects of TES^{15kHz}-TI^{1Hz} on SWA between first and last intervention night are positively associated with subjective ratings of restorative sleep.

Conclusions: To our knowledge, this is the first study demonstrating that TES-TI enhances SWA and potentially its restorative function.

Plain Language Summary

Slow waves are signature patterns of electrical activity indicative of deep sleep. They play an important role in the ability of sleep to be and feel restorative. Boosting slow wave activity has been shown to be beneficial for memory and cognition but the current techniques for doing so have limitations. Here, we use a non-invasive technique—Transcranial Electrical Stimulation with Temporal Interference (TES-TI)—that overcomes these limitations and allows for sensation-free modulation of deep brain regions that can be performed with simultaneous electroencephalography (EEG) to record brain activity during sleep. The main findings support the ability of TES-TI to enhance slow wave activity during non-rapid eye movement sleep in healthy humans. Future studies that build upon this work by investigating the TES-TI mechanism of action and optimizing parameters will serve as important steps toward the utilization of TES-TI for the improvement of sleep.

ARTICLE IN PRESS

Introduction

During non-rapid eye movement (NREM) sleep, which comprises 75–80% of total time spent in sleep, individual slow waves are detected on electroencephalography (EEG) when many cortical neurons switch near-synchronously between ON periods of firing and OFF periods of silence [1]. Sleep slow waves are homeostatically regulated. Thus, slow wave activity (SWA, EEG power in 0.5–4 Hz range), a combined measure of the number and amplitude of slow waves, is high in early sleep, even higher after sleep deprivation, and declines in the course of sleep when sleep need is discharged [2-4]. SWA is maximal during the deepest stages of sleep. Slow waves are believed to mediate key restorative functions attributed to NREM sleep, including synaptic renormalization and memory consolidation [5-11]. Slow waves, in conjunction with spindles and sharp-wave ripples, may coordinate the reorganization of memories within the cortex [9-11]. Disrupted SWA is associated with worsened cognitive functioning, including poorer performance on visuomotor and perceptual learning tasks [12-14]. Conversely, the enhancement of SWA has been shown to improve cognitive performance in several domains, such as verbal fluency, working memory, and declarative memory [15-19].

Two interventions commonly used to enhance SWA are acoustic stimulation and transcranial electrical stimulation (TES) [13,15-20]. However, both techniques have limitations. Acoustic stimulation strong enough to elicit SWA can be close to the threshold for awakening the participant [13]. Conventional TES, which typically employs frequencies below 1 kHz, results in electrical artifacts during stimulation that prevent adequate evaluation of simultaneous EEG recordings, particularly at the stimulation frequency [18]. In addition, conventional TES stimulates broadly, affecting superficial regions with diminishing efficacy over deeper brain regions when using parameters that do not produce scalp discomfort [21].

An innovative neuromodulatory tool potentially able to overcome these limitations is Transcranial Electrical Stimulation with Temporal Interference (TES-TI), also called Temporal Interference Stimulation (TIS)[22] or interferential current stimulation [23-26]. It uses two or more high frequency alternating current carriers (e.g., 15 kHz and 15 kHz + 1 Hz) to produce "temporal interference," that is, amplitude modulation at the difference frequency (e.g., 1 Hz) capable of modulating neural activity at a targeted location in an individual's brain [22]. This approach achieves both depth of penetration and focality [22]. Moreover, TES-TI is steerable, in a way not easily attainable with other non-invasive neuromodulation techniques, by adjusting the current ratio of the two channel pairs [22]. Importantly, high frequency carriers allow for effective stimulation intensities without the participant perceiving any peripheral stimulation that could cause awakening from sleep [27,28]. While the exact mechanism by which TES-TI modulates neural activity is an area of active investigation [22,26,29,30], several studies have now implemented TES-TI with high frequency carriers (up to 20 kHz) in a safe and effective manner in humans [31-35]. For example, in healthy populations, reported effects include changes in connectivity [33,34,36] and/or behavior on various tasks, including motor learning, episodic memory, and spatial navigation [34-38]. Currently, less is known in clinical populations; however, preliminary evidence suggests potential benefits for individuals with Parkinson's disease or epilepsy [34,39]. To our knowledge, no study has reported on the use of TES-TI to promote sleep, and more specifically, to enhance SWA.

The current study is an interim analysis of data from the STRENGTHEN study that focuses on the effects of TES-TI during NREM sleep and uses data from simultaneously recorded high-density EEG (hd-EEG) and TES-TI during overnight sleep in a laboratory setting in healthy humans. TES^{15kHz}-TI^{1Hz} (15 kHz carrier, 1 Hz difference) targeted left ventromedial prefrontal cortical regions given evidence from source modeling [40] and invasive recordings [41] suggesting that these areas are a "hot spot" for slow wave generation. With hardware filters, simultaneous hd-EEG recording was obtained while TES^{15kHz}-TI^{1Hz} was delivered

during periods of NREM sleep in the first half of the night. The main results show that SWA increases during and after TES^{15kHz}-TI^{1Hz}. Low frequencies (SWA, theta) increase and high frequencies (sigma and beta) decrease with TES^{15kHz}-TI^{1Hz}. During stimulation, SWA is greater in TES^{15kHz}-TI^{1Hz} as compared to TES^{15kHz} (15 kHz carrier only). Lastly, the increases in SWA with TES^{15kHz}-TI^{1Hz} between first and last intervention nights are positively associated with improved ratings of restorative sleep quality. Altogether, these results provide evidence in support of the ability of TES^{15kHz}-TI^{1Hz} to enhance sleep SWA and potentially its restorative functions.

Methods

Study Design

Data used in this study were acquired as part of the ongoing STRENGTHEN clinical trial (ClinicalTrials.gov, NCT06267521, registration date: 02/12/2024), a single-blind, longitudinal study aimed at enhancing cognitive flexibility and emotion regulation. The study design includes Transcranial Electrical Stimulation with Temporal Interference (TES-TI) delivered during sleep in the lab as well as brief, daily meditation training (**Figure 1A**). Healthy participants (ages 18–50) were assigned in parallel to 1 of 4 groups: (Group 1) TES^{15kHz} (0 Hz difference frequency) 2 night per week and meditation; (Group 2) TES^{15kHz}-TI^{1Hz} (1 Hz difference frequency) 2 nights per week and sham meditation; (Group 3) TES^{15kHz}-TI^{1Hz} 1 night per week and meditation; (Group 4) TES^{15kHz}-TI^{1Hz} 2 nights per week and meditation (**Figure 1B**). For all participants, interventions during sleep in the lab occurred over four consecutive weeks. Participants were assigned to their treatment group following pre-intervention baseline assessment, with efforts made during non-random allocation to ensure group equivalence on key demographic variables, particularly age and sex. This matching approach mitigated potential confounds related to sex and aged-based differences in sleep. Participants were blinded to their experimental group, i.e. they did not know whether they were receiving TES^{15kHz} (Group 1) or TES^{15kHz}-TI^{1Hz} (Groups 2,3,4). Participants were reimbursed for their study participation. Neither participants nor the public were involved in the design, conduct, or reporting of this trial. All aspects of the study were approved by University of Wisconsin-Madison Institutional Review Board.

The current study reflects a mechanistic sub-study within the broader STRENGTHEN trial; it is an interim analysis that focuses on the effects of TES^{15kHz}-TI^{1Hz} during NREM sleep using data collected from the first five cohorts of the STRENGTHEN trial (from February 19, 2024, to December 31, 2024). Each cohort contained approximately 5-6 participants who, for logistical reasons, went through the various phases of the study as a group. The analyses presented here were not pre-specified in the formal clinical trial registration; however, they were part of the planned exploratory aims within the Institutional Review Board-approved protocol and were designed prior to data collection from the analyzed cohorts. Primary and secondary endpoints of the trial related to cognitive flexibility and emotion regulation will be the focus of later work; as such, data from post-intervention follow-up periods were not included in the current work. The analyses performed here were initiated after interim inspection of the data showed large effect sizes. To maximize statistical power, the current study used data from the first five cohorts to examine the effects of TES^{15kHz}-TI^{1Hz} on NREM sleep (N = 21, 1 Hz, targeting left ventromedial prefrontal cortex during NREM sleep episodes in the first half of the night) by comparing the baseline night with the first and last intervention nights regardless of the group. A comparison between TES^{15kHz}-TI^{1Hz} and TES^{15kHz} (i.e., directly assessing the potential effects of amplitude modulation) was also performed utilizing Group 1 participants from the first five cohorts (N = 7). More detailed information about statistical power and participant grouping can be found in the *Statistics and Reproducibility* section. Another goal of the

ARTICLE IN PRESS

STRENGTHEN clinical trial, to be reported in a subsequent publication, was the assessment of TES^{15kHz}-TI^{6Hz} (6 Hz, targeting retrosplenial cortex) during REM sleep episodes later in the night.

Participants

In total, twenty-eight participants (30.5 ± 9.9 years, 61.0% (N = 17) Female, N = 21 TES^{15kHz}-TI^{1Hz}, N = 7 TES^{15kHz}) from the first five cohorts of the STRENGTHEN study were included in the current study (**Figure 1C**). All participants were medically healthy, with no acute illness at the time of participation and no diagnosed chronic illness, including sleep disorders, or medications that may have influenced the outcome of the study. Participants had a baseline magnetic resonance imaging (MRI) scan and sleep night in the lab. The baseline sleep night did not include overnight stimulation. Participants were to be excluded if they had any neuroradiologist-identified structural abnormalities of the brain; no participants in the current work were excluded for this reason. Participant recruitment began with an online survey. Potential participants were then further screened by phone call to see if they met eligibility criteria. They then underwent additional screening and an informed consent discussion in person prior to potential enrollment in the study. In general, screening consisted of questions regarding demographics, availability, medical and mental health, medications, and sleep. Participants with responses meeting exclusion criteria were not included in the study. As part of screening, for example, participants were asked about current or prior diagnoses of Obstructive Sleep Apnea (OSA); if yes, the participant was excluded. Full eligibility criteria can be found on the ClinicalTrials.gov website. As part of the pre-intervention baseline sleep visit, sleep technicians monitored for sleep quality. During the baseline sleep visit, two participants had loud snoring, breath holding and gasping accompanied by periods of wake. Given concern for OSA and overall poor sleep that would preclude experiment completion, these two participants were withdrawn after their baseline visit (**Figure 1C**). All participants gave written informed consent in accordance with the University of Wisconsin-Madison Institutional Review Board.

Datasets Included

Baseline, first, and last intervention nights were utilized here; a future publication will report on all the intervention nights. In total, twenty-two first nights and twenty-seven last nights were included in subsequent analyses that evaluated effects of stimulation. Four first nights were excluded due to technical issues and two first nights were excluded due to poor sleep that precluded experiment completion (e.g., fewer than five out of ten intended stimulation protocols were completed). One last night was excluded due to technical issues. Analyses comparing baseline, first, and/or last intervention nights were restricted to participants with usable data across all nights. Further details about which datasets were included in the analyses can be found in Supplementary Figure 1.

Daytime Meditation Training

Meditation and sham meditation interventions were delivered via the Healthy Minds Program (HMP) smartphone app, which provides a comprehensive curriculum for well-being training based upon four pillars of well-being: awareness, connection, insight, and purpose [42,43]. The program includes didactic mini podcasts that provide the background science underlying each of the four well-being pillars, along with specific mental exercises–forms of procedural learning–that complement the declarative scientific content [42,43]. Participants assigned to the meditation intervention were guided through brief, daily meditation practice (5-30 minutes) and provided regular reminders of key practice goals several times

ARTICLE IN PRESS

each day. Each week focused on one of the four pillars of well-being. Participants assigned to the sham meditation intervention listened to didactic material only, without meditation instruction.

Nighttime Stimulation Procedure

Participants spent overnights in the sleep lab at the Wisconsin Sleep Center, where they were outfitted with a 256-channel hd-EEG net for recording brain activity and additional channels for recording polysomnography (PSG) data (electrooculography adjacent to lateral canthi, submental electromyography, and electrocardiography). Channels for performing TES-TI were embedded in the hd-EEG net, placed in lieu of recording channels. While the participant was awake, short stimulation protocols (15-seconds with 15-second ramping up/down periods) were performed with increasing current amplitudes (up to 5 mA zero-to-peak) to determine if a participant began to feel sensation on their scalp. The current amplitude was then lowered systematically and checked again such that the final current value of 5 mA chosen did not elicit any sensation. Then, the participant went to sleep, and a sleep technician performed stimulation protocols based on sleep features visible on the hd-EEG and PSG recordings (data visualization parameters in accordance with staging parameters found in the Sleep Staging section). Specifically, when NREM sleep was identified and stable (≥3 minutes), stimulation was delivered in 3-minute protocols with 15-second ramping up/down periods. Each protocol was separated by at least 6 minutes and repeated approximately ten times, in most cases confined to NREM sleep episodes during the first four hours after sleep onset. Participants were monitored throughout the night from a control room, and a sleep technician was available for communication at any time.

Sleep Quality Surveys

After each overnight in the sleep lab, participants completed the 9-question Restorative Sleep Questionnaire (REST-Q) survey, which was designed by a panel of expert sleep specialists to define and measure restorative sleep [44,45] and chosen here for its potential to link the perceived restorative effects of sleep with the SWA that may underlie these restorative effects. . They rated to what extent they felt tired, sleepy, in a good mood, rested, refreshed, ready to start the day, energetic, mentally alert, and grouchy on scales of 1 to 5 (1 = Not at all, 2 = A little bit, 3 = Some, 4 = Very much, 5 = Completely). An overall REST-Q score was calculated in line with [29]. Overall scores from after the first and last intervention nights were included in the analyses.

TES-TI Targeting

A standardized channel montage was used for all participants (channel 1: E20–E34, channel 2: E70–E95 of the hd-EEG net) targeting left ventromedial prefrontal cortical regions. Channel placement was first approximated using the Temporal Interference Planning Tool (TIP v1.0, IT'IS Foundation, Switzerland), in which an optimal channel configuration was chosen from the 10:10 system to target the left ventromedial prefrontal cortex with maximal intensity and minimal off-target stimulation [46,47]. TIP simulations were performed using the comprehensive MIDA head model, which details the electrical properties for different tissues in a twenty-nine-year-old healthy female volunteer [48]. For further confirmation, targeting was then verified using SimNIBS software (v4.1.0) that provided tools for electric field modeling with additional details including: an individual's MRI, and channel material, geometry, and position in the 256 hd-EEG system [49-51]. Modeling began with segmentation of an individual participant's T1 and T2 scans to extract electrical properties of different tissues. Segmentation and meshing were performed using the *charm* function. The participant's head model was then aligned to a template 256-channel hd-EEG net [51]. Next,

ARTICLE IN PRESS

electric fields were simulated accounting for channel properties (see *TES-TI Stimulation*), a current value of 5 mA zero-to-peak, and location in the 256-channel hd-EEG net extrapolated from the 10:10 system locations used in TIP simulations. Simulation of the temporal interference field (V/m) was implemented using the function *get_maxTI* that calculates the maximal modulation amplitude of the difference frequency using the equation described in [22,51]. The interference field values obtained in grey matter were then extracted and plotted over the individual's T1 scan as well as over a standardized atlas (MNI152) for visualization using SimNIBS and AFNI (Analysis of Functional NeuroImages) software [52,53].

Overall, simulations performed in SimNIBS with individualized head models agreed with those performed in TIP using the standardized MIDA head model. Based on these simulations using individualized head models, across all TES^{15kHz}-TI^{1Hz} participants (N = 21), maximal intensity values in left ventromedial prefrontal cortex grey matter were 0.82 ± 0.09 V/m, ranging 0.62–0.99 V/m and average intensity values were 0.46 ± 0.05 V/m, ranging 0.36–0.52 V/m. Of note, the channel configuration used for two TES^{15kHz}-TI^{1Hz} participants differed by one channel (E94 instead of E95); however, their data was included given that electric field simulations for both configurations were highly similar.

TES-TI

Four silver-silver chloride stimulating channels (12.6 mm outer diameter, 8.0 mm inner diameter, 2.2 mm width) with 1.5-meter cable length were embedded into the hd-EEG net, attached to the participant's scalp with conductive paste (Ten20), and then connected to the TI Brain Stimulator for Research (TIBS-R v3.0, TI Solutions AG, Switzerland). Electrode impedances were monitored throughout the experiment and served as an indicator for the need to adjust electrodes; substantial increases in impedance (to greater than 6500 Ohm) indicated poor positioning and a need for adjustment. Adjustments were targeted for when a participant entered a light stage of sleep (i.e., N1) or wake. Adjustments consisted of applying additional Ten20 conductive paste and/or measures to improve electrode adherence to the scalp. Overall, adjustments were infrequent, as out of the 49 stimulation nights analyzed, only 4 nights had adjustments, which occurred one or two times during periods of wake. Average impedances were 4590 ± 110 Ohm for channel 1 and 5020 ± 600 Ohm for channel 2. TES-TI protocols during NREM sleep had the following parameters: 15,000 Hz carrier frequency, 1 Hz difference frequency, sinusoidal waveform, 5 mA zero-to-peak, 3-minute duration with 15-second ramping up/down periods. Channel 1 used a 15,000 Hz frequency and channel 2 used a 15,001 Hz frequency. As a higher carrier frequency lowered impedance at the electrode-scalp interface, a 15,000 Hz carrier frequency was chosen to mitigate the possibility of sensations being felt by participants during sleep. Actual, average current delivered was 5.21 ± 0.21 mA for channel 1 and 5.06 ± 0.19 mA for channel 2 as reported by the TIBS-R device. Programming of the TIBS-R device was performed using its Python software.

hd-EEG Data Acquisition

The hd-EEG system from MagStim Electrical Geodesics, Inc. (EGI) consisted of a hd-EEG net, an amplifier (NA 400), and a physiological input box. Each net had 256 silver-silver chloride electrodes and was appropriately sized to each individual participant. In cases where the stimulating electrodes were very close to the hd-EEG recording electrodes, e.g., small net sizes, surrounding recording electrodes were not gelled to avoid the possibility of bridging between stimulating and recording electrodes. Nets were then connected to EGI amplifiers that interface with EGI's Net Station Acquisition software (v5.4.2) for real-time data visualization. All recording electrode impedances were kept below 50,000 Ohm, with the reference electrode below 5,000 Ohm, as measured at the start of the recording. The physiological input box was used

ARTICLE IN PRESS

to collect polysomnography data (electrooculography, electromyography, and electrocardiography). In addition, data from the TIBS-R trigger was input into the physiological input box. The optical trigger box output a 5 V square wave signal with the onset and offset of stimulation and, when synchronized to hd-EEG recordings, allowed for offline identification of stimulation intervals. All data were collected at a 500 Hz sampling rate. The total number of hours of EEG data acquired across the baseline, first, and last nights utilized in these analyses was 7.99 ± 0.75 hours per night per participant.

Hardware filters specifically designed for the TIBS-R device allowed for simultaneous TES-TI and hd-EEG recording. A low-pass filter (7th order, 100 Hz cutoff) was placed in the path of the hd-EEG amplifier input such that signals from the hd-EEG net were filtered before they reached the amplifier. A high-pass filter (4th order, 250 Hz cutoff) was placed in the path of the TIBS-R output such that intermodulation products and low-frequency noise generated by the TIBS-R were filtered before they reached the stimulating electrodes. Both hardware filters were used to allow for simultaneous TES-TI stimulation and hd-EEG recording.

MRI Data Acquisition

MRI data were collected using a 3 Tesla MAGNUS (Microstructure Anatomy Gradient for Neuroimaging with Ultrafast Scanning, GE Healthcare) head-only MRI scanner. The head coil used was a 32-channel head radio frequency (RF) array (Nova Medical, Wakefield, MA). Structural images were acquired using T1- and T2-weighted images, with 0.8 mm isotropic voxels, and the following parameters. T1-weighted: sequence = MP-RAGE (Magnetization-Prepared Rapid Gradient-Echo), repetition time (TR) = 2000 ms, echo time (TE) = 3 ms, inverse time (TI) = 1100 ms, flip angle = 8 degrees, field of view (FOV) = 256 x 256 mm^2, matrix size = 320 x 320 pixels, resolution = 0.8 mm x 0.8 mm x 0.8 mm, number of slices = 240, acquisition time = 4 min. T2-weighted: sequence = CUBE-T2, TR = 2500 ms, TE = 90 ms, echo train length (ETL) = 120, FOV = 256 x 256 mm^2, matrix size = 320 x 320 pixels, resolution = 0.8 mm x 0.8 mm x 0.8 mm, number of slices = 240, acquisition time = 4 min. The structural MRI data were converted into NIfTI format using the open-source tool *dcm2niix*. Both T1- and T2-weighted images were defaced for all participants using the open-source Python-based defacing utility tool, *pydeface*.

Sleep Staging

Sleep staging was performed manually in accordance with the American Academy of Sleep Medicine guidelines and as follows by a registered polysomnographic technician [54]. Electrooculography, electromyography and 6 hd-EEG channels that approximate 10:20 locations F3, F4, C3, C4, O1, O2 were used for staging. Hd-EEG data were filtered using MATLAB's *filtfilt* function with design: 4^{th} order infinite impulse response filter band-passed 1–30 Hz. Electromyography data were filtered using MATLAB's *filtfilt* function with design: 4^{th} order infinite impulse response filter band-passed 1–100 Hz followed by a notch filter: 4^{th} order infinite impulse response filter stop band 59-61 Hz. CountingSheepPSG (v1.4.5) MATLAB software was then used to perform staging in 30-second epochs and calculate sleep metrics such as Total Sleep Time, Sleep Onset Latency (to Stage 1), Wake After Sleep Onset, and others. Number of arousals and arousal index (number of arousals per hour) were quantified in line with AASM guidelines [54]. Number of awakenings was also included and refers to the number of times the stage transitioned from sleep to wake. Nonparametric statistical tests were used to evaluate for potential changes in these metrics across participant groups (Wilcoxon rank sum) and within participants, across intervention nights (Friedman test).

hd-EEG Preprocessing

ARTICLE IN PRESS

hd-EEG data preprocessing was performed using MATLAB (v2023b) and EEGLAB (v2025.0.0) [55]. hd-EEG data were band-pass filtered 0.5–40 Hz using EEGLAB's finite impulse response filter function, *pop_eegfiltnew*. Only 30-second NREM epochs staged 2 or 3 were included in spectral power analyses.

hd-EEG Artifact Rejection

Semi-automated artifact rejection was performed to remove channels and epochs containing artifactual activity (e.g., high-frequency noise, interrupted contact with the scalp) [56-58]. Specifically, a Fast Fourier Transform (FFT) was used to calculate spectral power in low (0.5–4 Hz) and high (20–30 Hz) frequency ranges for 6-second NREM epochs. For each channel, automatic thresholds were calculated at the 99th percentile and then plotted and visually inspected. If epochs with substantially greater low- or high-frequency power did not exceed the automatic threshold, the threshold was lowered. All epochs exceeding the threshold were then removed. Removed epochs (due to artifact or a sleep stage that was not NREM 2 or 3) were replaced with NaN values to maintain the temporal structure of the data but were not included in the spectral power calculations.

Channels in which artifacts affected most of the recording were removed. Additional spectral- and topographic-based procedures were used to identify and remove channels with distinctly greater power relative to neighboring channels. On average, 74% (189 ± 23) of the 256-hd EEG channels remained on intervention nights. A final visual review of the hd-EEG data was performed to remove any remaining channels and epochs with artifactual activity.

To increase the signal-to-noise ratio, analyses were restricted to 185 scalp channels (excluding neck and face channels). Any removed channels, including channels that were not gelled, within the scalp 185 channels were interpolated using spherical spline interpolation via the *eeg_interp* function. All channel data was then re-referenced to the average of the final 185 channels. For visualization only, topographies were plotted using EEGLAB's *topoplot* function with a decreased radius (plotrad = 0.51); all 185 channels were included in analyses.

hd-EEG Alignment

Timing of TES-TI throughout the night was determined based on hardware trigger signals in agreement with timestamps recorded at the start and end of individual stimulation protocols. Time periods included a baseline PRE stimulation period 3-minutes prior to the start of stimulation, a STIM period including a 15-second ramp up, 3-minute stimulation, and 15-second ramp down, and a POST stimulation period 3-minutes after the ramp down. Analyses comparing STIM and PRE or POST intervals excluded the ramping interval to allow for equal 3-minutes comparisons.

hd-EEG Spectral Power Analyses

For each hd-EEG channel, power spectral density (PSD) was calculated with Welch's method using 6-second windows with 90% overlap for a 0.167 Hz step size. PSD values were then averaged over frequencies to calculate band power (e.g., SWA, 0.5–4 Hz). Band power was normalized to account for differences between participants and night-to-night variability within participants [59]. For each participant and each night, the band power of interest (e.g., SWA) for each channel in PRE, STIM, and POST periods was divided by the average band power (e.g., SWA) during NREM sleep throughout the entire night to obtain a relative change (shown as a percent) from the mean overnight band power [59]. Canonical frequency bands were defined as follows, SWA: 0.5–4 Hz, theta: 4–8 Hz, alpha: 8–12 Hz, low sigma: 9–12 Hz, high sigma: 12–16 Hz, beta: 16–25 Hz, gamma: 25–40 Hz. The main analyses were also repeated using a

ARTICLE IN PRESS

narrower frequency band surrounding SWA, 0.5-2 Hz, and the results were qualitatively similar to the broader 0.5-4 Hz band.

Statistics and Reproducibility

Summary statistics for the main figures, including sample sizes and effect sizes (Cohen's d), can be found in Supplementary Table 4.

Hypothesis Testing

Descriptive statistics in the text are reported as mean ± standard deviation. Prior to performing any statistical tests, data were evaluated for normality using the Shapiro-Wilk test (*swtest* in MATLAB, v2023b). If data distributions were normal, parametric tests were used; if data distributions were not normal, nonparametric tests were used. All statistical tests were two-sided.

Correction for Multiple Comparisons

To assess for statistical significance in the context of multiple comparisons, the Benjamini-Yekutieli procedure was used to correct families of comparisons to a false discovery rate of 5% (*fdr_bh* in MATLAB). Comparisons were grouped into families based on conceptual similarity and corrections were applied within each family. P-values reported in the text are adjusted according to this procedure; if adjustment resulted in a number greater than 1, p-values are reported as $p > 0.999$. Both the original unadjusted p-values and the reported adjusted p-values can be found in Supplementary Table 4. For analyses that do not report adjusted p-values (e.g., age, sex, number of stimulation protocols, etc.), tests were conceptually isolated and not considered to be part of a family requiring correction for multiple comparisons.

Statistical Power

Statistical power calculations were performed using the *pwr* functions in R (v4.5.2) for t-tests with a two-sided alpha at 0.05 and using effect sizes observed in the sample. The primary findings that used data from participants that received the TES^{15kHz}-TI^{1Hz} intervention were highly powered (e.g., Figure 3, STIM-PRE, N = 21, Cohen's d = 1.45, $\beta = 0.99$, $\alpha = 0.05$, two-sided paired samples t-test). The comparison performed between TES^{15kHz}-TI^{1Hz} participants and TES^{15kHz} participants was moderately powered, but a significant difference was nevertheless detected with a large effect size (Figure 4A, B, TES^{15kHz}-TI^{1Hz} N = 21, TES^{15kHz} N = 7, Cohen's d=1.08, $\beta = 0.66$, $\alpha = 0.05$, two-sided independent samples t-test). Preliminary findings pertaining to only the TES^{15kHz} group, given the small sample size, were included in the Supplementary Information; the results of TES^{15kHz} group analyses should be considered exploratory and hypothesis-generating rather than confirmatory.

Cluster-Based Statistics for Topographic Analyses

For topographic comparisons, a nonparametric cluster-based statistical approach using a suprathreshold cluster analysis to control for multiple comparisons was implemented [60-62]. For each permutation (N=5000), new datasets were generated with randomly relabeled conditions from the original data. Then, a selected statistical test (e.g., t-test or Spearman correlation) was performed and clusters were determined based on neighboring channels exceeding the critical value for a given two-tailed test distribution, degrees of freedom, and alpha of 0.05. The maximal size of resulting clusters was used to build a cluster size distribution across all permutations. The critical cluster size threshold was defined as the 95^{th} percentile of this distribution. For the empirical comparison, only channels that exceeded the critical value and were

ARTICLE IN PRESS

located within a cluster larger than the critical cluster size threshold were considered significant [60,61]. The number of significant clusters, total number of significant electrodes, and mean p-value ($\bar{p}$) of those significant electrodes are reported; channels with significant responses are shown as white dots in figures. If no significant clusters were identified, the mean p-value ($\bar{p}$) across all electrodes is reported.

Linear Mixed Effects (LME) Model for Participant Grouping

A linear mixed effects (LME) model was used to assess for any differences across subgroups that received the TES^{15kHz}-TI^{1Hz} intervention. In general, as described in [63], the LME was fit with numerical maximum likelihood estimation using the *lmer* function of the *lme4* package in R. In general, the model related the response variable (y) to experiment and the covariate of interest (x) as fixed effects with an interaction term, and participant as a random effect (that is, 'M1 = $y \sim x$ * experiment + (1 | participant)'). We then tested the hypothesis that there was no interaction between x and the experiment by fitting a model with the interaction term removed (that is, 'M2 = $y \sim x$ + experiment + (1 | participant)') and performing an asymptotic likelihood ratio test to compare the full and reduced models. In all cases, residual plots were examined for evidence against the assumptions of constant variance and normality. If no significant interaction was found, we tested for a main effect of the primary covariate by fitting a model with that term removed (that is, 'M3 = $y \sim$ experiment + (1 | participant)') and performed an asymptotic likelihood ratio test to compare this model with the one including the covariate ('M2'). Cohen's f^2 was used as a measure of effect size and was calculated as in [63].

Specifically, for these analyses, SWA was the response variable, and TES^{15kHz}-TI^{1Hz} subgroup (Groups 2, 3, or 4) and period (PRE, STIM, POST) were fixed effects. Two separate models were applied, one for the first night and one for the last night.

Least Absolute Shrinkage and Selection Operator (LASSO) Model for Sleep Quality

A predictive modeling approach was used to identify potential factors associated with REST-Q sleep quality ratings. Specifically, a regression analysis was performed using Least Absolute Shrinkage and Selection Operator (LASSO) estimation with 5-fold cross-validation to select model hyperparameters (*glmnet* function in R). The LASSO is a regularization technique that drives coefficient estimates to zero for marginal inputs, resulting in a sparse regression that identifies which model inputs improve the prediction of the model outputs. Power averaged across all channels in SWA, theta, beta, low sigma, and high sigma bands during STIM-PRE and POST-PRE periods (independent variables) were used as predictors for overall REST-Q ratings (dependent variable). Models were fit on first and last night data as well as the difference between last and first nights to assess for longitudinal changes within-participant. For the models, λ_min values are reported as they represent the level of regularization that minimized cross-validated prediction error. Mean squared error (MSE) for the held-out test folds is also reported. To visualize potential predictive relationships, linear regression models were used, and the line of best fit ($y = \beta_1 * x + \beta_0$) and R^2 values are reported. To explore whether the predictive power in the observed data was spatially localized, for descriptive purposes, R^2 values from the linear regression models were plotted topographically. The predictive modeling approach does not use the null hypothesis testing framework; instead, a training-testing split of the data via cross-validation plays the role of preventing overfitting and ensuring that the results for each model cannot be explained by random variation. Nevertheless, in the context of multiple models, findings should be considered preliminary rather than confirmatory.

ARTICLE IN PRESS

Results

Twenty-eight participants (30.5 ± 9.9 years of age, 61% (N = 17) Female, N = 21 TES^{15kHz}-TI^{1Hz}, N = 7 TES^{15kHz}) from the first five cohorts of the STRENGTHEN clinical trial were included in the current study. As described in the Methods, participants were assigned to one of four groups, receiving interventions over the course of four weeks (**Figure 1A,B**). Twenty-one participants (Groups 2,3,4) received TES^{15kHz}-TI^{1Hz} and seven other participants (Group 1) received TES^{15kHz} (**Figure 1B,C, Supplementary Figure 1**). All participants had a baseline overnight with polysomnography (PSG) and hd-EEG recordings. Afterwards, overnight interventions consisted of PSG, hd-EEG, and stimulation. Hardware filters allowed for simultaneous hd-EEG recordings and stimulation (**Figure 2A**). TES^{15kHz}-TI^{1Hz} protocols performed during NREM sleep had the following parameters: 15,000 Hz carrier frequency, 1 Hz difference frequency, sinusoidal waveform, 5 mA zero-to-peak, 3-minute duration with 15-second ramping up/down periods (**Figure 2B,D**). Electric field modeling was used to target the left ventromedial prefrontal cortical region. The montage chosen (channel 1: E34–E20, channel 2: E70–E95) generated a theoretical electric field in which the amplitude-modulated (temporal interference) field exceeded 0.7 V/m in the target region when simulated for a representative participant (**Figure 2C**). Across all TES^{15kHz}-TI^{1Hz} participants (N = 21), maximal intensity values in left ventromedial prefrontal cortex grey matter were 0.82 ± 0.09 V/m, ranging 0.62–0.99 V/m. Average intensity values were 0.46 ± 0.05 V/m, ranging 0.36–0.52 V/m. Stimulations occurred in three-minute protocols repeated ten times during NREM sleep identified online by sleep technicians (**Figure 2D**). For most nights, stimulations were completed within the first four hours from

ARTICLE IN PRESS

sleep onset, as endogenous SWA is typically high during this timeframe (**Figure 2D**). Stimulation parameters were the same across groups except that TES^{15kHz} had a difference of 0 Hz.

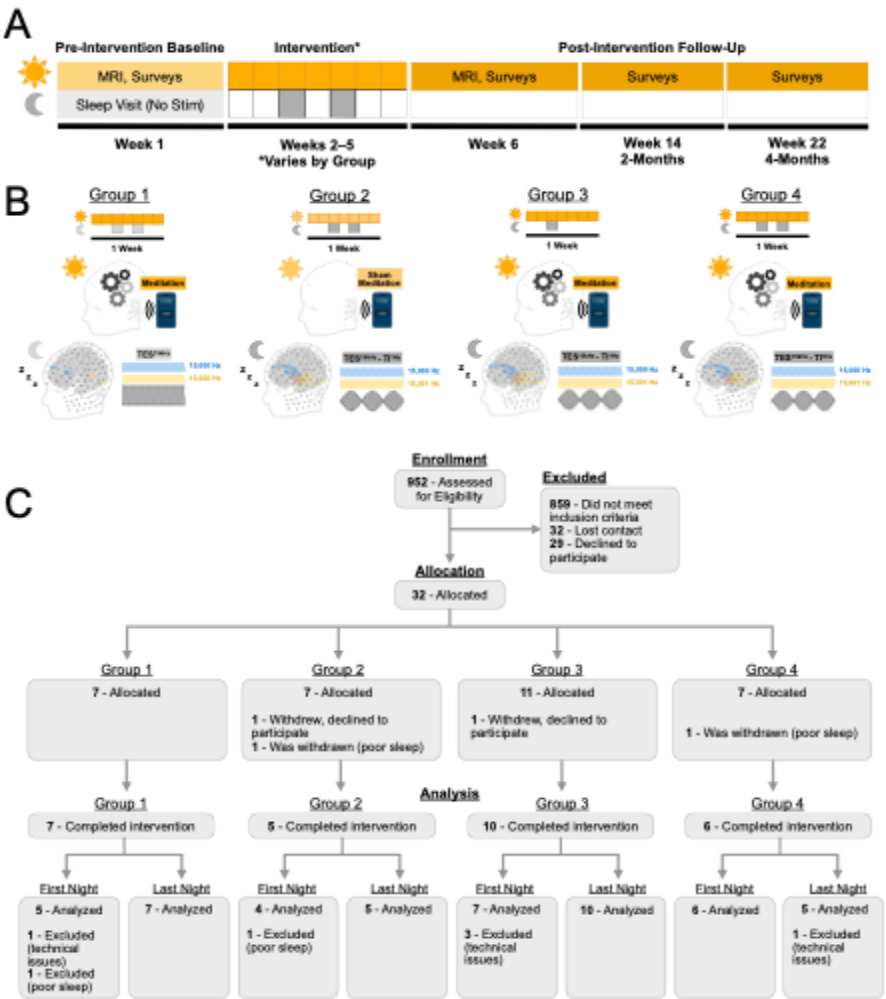

Figure 1. STRENGTHEN study overview. A. *Timeline of events for study participants divided into daytime (Top, orange) and nighttime (Bottom, grey) events. Pre-intervention baseline events consisted of surveys, a Magnetic Resonance Imaging (MRI) session, and overnight sleep visit (no stimulation performed). The intervention period lasted 4-weeks and consisted of interventions that varied according to group assignment. All groups performed meditation (or sham meditation) training daily; stimulation interventions occurred once or twice per week at night. Post-intervention follow-up events consisted of an MRI and surveys, which were repeated at 2 months and 4 months.* ***B.*** *Interventions varied according to assigned group (non-random allocation, parallel assignment). Group 1 performed meditation training daily and received Transcranial Electrical Stimulation (TES^{15KHz}) twice per week at night. Group 2 performed sham meditation daily and received Transcranial Electrical Stimulation with Temporal Interference (TES^{15KHz}-TI^{1Hz}) stimulation twice per week at night. Group 3 performed meditation training daily and received TES^{15KHz}-TI^{1Hz} stimulation once per week at night. Group 4 performed meditation training daily and received TES^{15KHz}-TI^{1Hz} stimulation twice per week at night. TES^{15KHz}-TI^{1Hz} used 15 kHz carrier frequency and 1 Hz difference frequency; TES^{15KHz} used only a 15 kHz carrier frequency. More information about TES-TI can be found in Figure 2.* ***C.*** *Participant flow diagram for the data collection period from February 19, 2024 to December 31, 2024. Thirty-two participants met inclusion criteria and were allocated to intervention groups. Two participants withdrew themselves from*

the study after their baseline assessments. Two participants were withdrawn by study personnel after evaluation of their baseline sleep visit showed poor sleep with concern for possible Obstructive Sleep Apnea. All remaining allocated participants completed the intervention and follow-up activities. For the analysis, numbers of participants in each group, for each night, are listed. Further information can be found in the Datasets Included section of the Methods and Supplementary Figure 1.

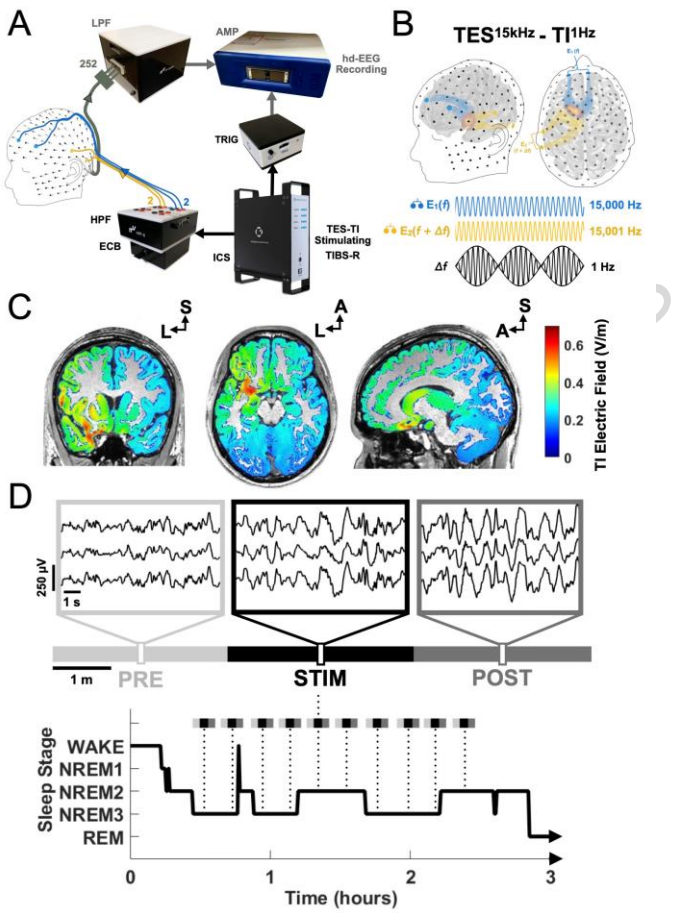

Figure 2. TES-TI overview. A. *The Transcranial Electrical Stimulation with Temporal Interference (TES-TI) system comprised the Temporal Interference Brain Stimulator for Research (TIBS-R) with components including the Intelligent Current Source (ICS), electrode connector box (ECB), and high-pass filter (HPF). Current was delivered through two pairs of stimulating electrodes (four electrodes total) embedded in the hd-EEG net. All other hd-EEG recording channels (252) passed through a low-pass filter (LPF) before reaching the recording amplifier (AMP). The dual HPF and LPF system allowed for simultaneous TES-TI and hd-EEG recording. Trigger (TRIG) outputs from the TIBS-R allowed for identification of when stimulation occurred.* ***B****.* TES^{15kHz}-TI^{1Hz} *consisted of one pair of electrodes delivering high frequency alternating current (E_1: 15,000 Hz) and the other pair delivering high frequency alternating current with an offset (E_2: 15,0001 Hz) to create amplitude modulation at the difference frequency (1 Hz) deep in the brain.* ***C****. Simulated temporal interference (TI) electric field in grey matter for an individual participant. Maximum TI electric field values occurred in deep, left ventromedial prefrontal cortical regions with values exceeding 0.7 V/m.* ***D****. (Top) A single stimulation protocol with three-minute periods before (PRE), during (STIM), and after (POST) stimulation. Three channels of example EEG data during ten seconds within each three-minute period shown. (Bottom) Representative example of the set of stimulations during NREM sleep, with ten stimulations occurring within the first hours after sleep onset.*

ARTICLE IN PRESS

Baseline, first, and last intervention nights were included in the current study. In total, twenty-two first nights (17 TES^{15kHz}-TI^{1Hz}, 5 TES^{15kHz}) and twenty-seven last nights (20 TES^{15kHz}-TI^{1Hz}, 7 TES^{15kHz}) were used in these analyses (**Supplementary Figure 1A**). Analyses comparing baseline, first, and last intervention nights were restricted to only participants with usable data on all nights (**Supplementary Figure 1B**,16 TES^{15kHz}-TI^{1Hz}, 5 TES^{15kHz}).

Across all participants, the age range was 19–49 years, race was 85.7% White, 14.3% Asian, and ethnicity was 96.4% non-Hispanic, 3.6% Hispanic, with no statistically significant differences in age or sex between TES^{15kHz}-TI^{1Hz} and TES^{15kHz} (**Table 1**). Sleep characteristics during the baseline night also did not differ between TES^{15kHz}-TI^{1Hz} and TES^{15kHz}, indicating adequate allocation of participants between groups (**Table 2**).

	TES^{15kHz} - TI^{1Hz}	TES^{15kHz}	Test Statistic (W or T), p-value
Number of Participants	21	7	
Age (yrs)	31.5 ± 10.0	27.4 ± 9.8	(W) 319.5, 0.441
Sex (%Female)	57.1	71.4	(X^2) 0.45, 0.503

Table 1. Basic demographics*. TES^{15kHz}-TI^{1Hz} and TES^{15kHz} participants show no statistically significant differences in age (two-sided Wilcoxon rank sum test) or sex (two-sided chi-squared test). Mean ± standard deviation.*

ARTICLE IN PRESS

ARTICLE IN PRESS

	TES^{15kHz} - TI^{1Hz}	TES^{15kHz}	Test Statistic (W or T)	p-value
Total Sleep-Wake Period (hr)	8.18 ± 0.94	7.62 ± 1.10	(W) 328.0	0.222
Total Sleep Time (hr)	6.83 ± 0.87	6.52 ± 1.25	(W) 311.5	0.730
Sleep Onset Latency (min)	23.10 ± 11.92	25.93 ± 14.00	(W) 293.5	0.577
REM Latency (hr)	1.97 ± 0.70	2.42 ± 0.53	(W) 272.0	0.089
Sleep Efficiency (%)	83.81 ± 8.58	85.49 ± 10.85	(W) 286.0	0.340
Number of Arousals	64 ± 36	62 ± 53	(W) 320.0	0.426
Arousal Index (arousals / hr)	9.29 ± 4.98	9.46 ± 7.28	(W) 314.0	0.633
Number of Awakenings	21 ± 9	17 ± 13	(W) 332.0	0.151
Wake After Sleep Onset (min)	57.71 ± 45.11	39.64 ± 37.23	(W) 326.0	0.265
Stage N1 (%)	4.63 ± 2.89	4.39 ± 4.52	(W) 320.0	0.426
Stage N2 (%)	60.58 ± 9.00	61.11 ± 7.03	(W) 298.0	0.750
Stage N3 (%)	14.00 ± 6.03	14.33 ± 5.64	(W) 301.0	0.874
Stage REM (%)	20.79 ± 5.34	20.17 ± 3.89	(W) 312.0	0.710
Whole-Night SWA (dB / Hz)	12.28 ± 2.41	11.72 ± 2.37	(T) 0.53	0.598
First 4hr SWA (dB / Hz)	12.17 ± 2.69	11.74 ± 2.55	(T) 0.37	0.717

Table 2. Baseline sleep characteristics. *TES^{15kHz}-TI^{1Hz} (N = 21) and TES^{15kHz} (N = 7) participants show no statistically significant differences in any sleep characteristics during the baseline night (two-sided Wilcoxon rank sum test). Mean ± standard deviation. Unadjusted p-values shown, when corrected for multiple comparisons using the Benjamini-Yekutieli procedure, all adjusted p-values were > 0.999. REM: Rapid Eye Movement, SWA: Slow Wave Activity.*

TES^{15kHz}-TI^{1Hz} preserves sleep architecture.

We compared sleep architecture metrics across baseline, first, and last intervention nights for those TES^{15kHz}-TI^{1Hz} participants with usable data on all nights (**Table 3**, TES^{15kHz}-TI^{1Hz} N = 16, Friedman tests, X^2, df = 2). There is a weak main effect of night on Total Sleep Time; however, it is not significant after correction for multiple comparisons (X^2 = 6.12, unadjusted p = 0.047, adjusted p > 0.999). There are no significant differences in any other sleep characteristics. Notably, there are no differences in metrics related

ARTICLE IN PRESS

to wake, including the number of arousals, arousal index, number of awakenings, or time spent awake after sleep onset. In addition, participants did not report feeling the stimulation during the night.

SWA (power spectral density, PSD in 0.5–4 Hz range) was quantified throughout each entire night then averaged across channels for each participant. There is no main effect of night (baseline, first, or last) on whole-night SWA (**Table 3,** TES^{15kHz}-TI^{1Hz}: N = 16, one-way repeated measures ANOVA, F, df = 2). Similar results were found when SWA was measured during the first four hours after sleep onset; this early SWA did not differ between baseline, first, or last nights (**Table 3**). Additionally, the number of stimulation protocols completed during NREM sleep did not differ between first and last nights (First = 10 ± 2, Last = 9 ± 1, W = 29.0, p = 0.910; two-sided Wilcoxon signed rank test). These comparisons were also repeated for the TES^{15kHz} group, but given the small samples size, results should be considered exploratory and hypothesis-generating (**Supplementary Table 1**).

	Baseline Night	First Night	Last Night	Test Statistic (X^2 or F)	p-value
Total Sleep-Wake Period (hr)	8.06 ± 0.99	8.25 ± 0.85	8.12 ± 0.78	(X^2) 0.88	0.646
Total Sleep Time (hr)	6.70 ± 0.83	7.04 ± 0.69	6.92 ± 0.79	(X^2) 6.12	0.047†
Sleep Onset Latency (min)	22.97 ± 11.89	23.44 ± 13.38	21.50 ± 15.39	(X^2) 2.51	0.285
REM Latency (hr)	1.86 ± 0.70	2.06 ± 0.76	1.93 ± 0.77	(X^2) 3.50	0.174
Sleep Efficiency (%)	83.62 ± 8.89	85.65 ± 6.65	85.33 ± 7.27	(X^2) 1.12	0.570
Number of Arousals	57 ± 26	69 ± 34	64 ± 31	(X^2) 1.24	0.538
Arousal Index (arousals / hr)	8.54 ± 3.95	9.80 ± 4.60	9.42 ± 5.12	(X^2) 0.88	0.646
Number of Awakenings	21 ± 7	21 ± 8	20 ± 8	(X^2) 1.76	0.414
Wake After Sleep Onset (min)	58.19 ± 47.17	48.56 ± 36.60	50.13 ± 36.78	(X^2) 2.13	0.345
Stage N1 (%)	4.07 ± 1.85	3.96 ± 2.94	4.07 ± 3.71	(X^2) 0.38	0.829
Stage N2 (%)	61.49 ± 9.83	61.88 ± 5.76	60.03 ± 5.65	(X^2) 0.38	0.829
Stage N3 (%)	13.75 ± 6.40	13.50 ± 6.35	12.62 ± 6.31	(X^2) 0.88	0.646
Stage REM (%)	20.70 ± 5.73	20.66 ± 2.91	23.28 ± 3.79	(X^2) 1.62	0.444
Whole-Night SWA (dB / Hz)	12.34 ± 2.71	12.12 ± 2.66	12.21 ± 2.69	(F) 1.16	0.327
First 4hr SWA (dB / Hz)	12.54 ± 2.69	12.37 ± 2.75	12.45 ± 2.90	(F) 0.50	0.611

ARTICLE IN PRESS

Table 3. Sleep characteristics across nights in TES^{15kHz}-TI^{1Hz}. *Across baseline, first, and last nights, TES^{15kHz}-TI^{1Hz} (N = 16) participants show no significant differences in any sleep characteristics after correction for multiple comparisons (Friedman test or one-way repeated measures ANOVA, Benjamini-Yekutieli procedure to correct for multiple comparisons). Mean ± standard deviation. Unadjusted p-values shown, when corrected for multiple comparisons, all adjusted p-values were > 0.999. †Total Sleep Time is not significant after correction for multiple comparisons (X^2 = 6.12, unadjusted p = 0.047, adjusted p >0.999). REM: Rapid Eye Movement, SWA: Slow Wave Activity.*

SWA increases during and after TES^{15kHz}-TI^{1Hz}.

We measured SWA in the immediate three-minutes before (PRE), during (STIM), and after (POST) TES^{15kHz}-TI^{1Hz} stimulation and calculated the differences between time periods (**Figure 3A**). SWA was normalized (%SWA) to account for SWA differences between participants and night-to-night variability within participants (see Methods, hd-EEG Spectral Power Analyses). Since SWA changes were consistent on the first and last intervention nights (**Supplementary Figure 2**), we averaged Δ%SWA across the two nights for each participant (**Supplementary Figure 1**). We also included participants (N=5) with only one intervention night of usable data to increase statistical power.

Overall, we find a significant difference in the all-channel average SWA across PRE, STIM, and POST periods (N = 21, df = 2, F = 30.95, p = 7.54×10^{-9}, one-way repeated measures ANOVA). We find a global (across all channels) increase in SWA during the stimulation as compared to before stimulation (**Figure 3A**, STIM-PRE, N = 21, t = 6.64, p = 4.97×10^{-6}, d = 1.45; two-sided paired samples t-test). A global increase in SWA is also present after stimulation compared to before stimulation (**Figure 3A**, POST-PRE, N = 21, t = 7.46, p = 1.86×10^{-6}, d = 1.63; two-sided paired samples t-test). There are no significant differences between the periods after (POST) stimulation and those during (STIM) stimulation in the average across all channels (**Figure 3A**, POST-STIM, N = 21, t = 0.63, p = 0.982, d = 0.14, two-sided paired samples t-test). To identify statistically significant topographic changes at the level of individual channels, we implemented a nonparametric cluster-based statistical approach using a suprathreshold cluster analysis to control for multiple comparisons. The results of this topographical analysis confirm the results at the global level, i.e. SWA increases across all channels during stimulation and the increase persists to a similar degree after, with no significant differences between the STIM and POST periods, despite a higher T-statistic in frontal regions in the POST period (**Figure 2B,** STIM-PRE: 1 positive cluster, 185 significant electrodes, $\bar{p} = 1.92 \times 10^{-5}$; POST-PRE: 1 positive cluster, 185 significant electrodes, $\bar{p} = 6.98 \times 10^{-6}$; POST-STIM: 0 clusters, 0 significant electrodes, $\bar{p} = 0.538$). A similar pattern of increases during and after stimulation are found when using a narrower frequency band surrounding SWA, 0.5-2 Hz (**Supplementary Figure 3A**). Analyses were also repeated for the TES^{15kHz} group, but given the small samples size, results should be considered exploratory and hypothesis-generating (**Supplementary Figure 4**).

To investigate potential differences across subgroups that received the TES^{15kHz}-TI^{1Hz} intervention (Groups 2,3,4), a linear mixed effects model (LME) was applied for first and last nights separately. SWA was the response variable, TES^{15kHz}-TI^{1Hz} subgroup and period (PRE, STIM, POST) were fixed effects. We find no significant interaction between subgroup and period (First: $f^2 = 0.16$, p = 0.079; Last: $f^2 = 0.07$, p = 0.571) and find no main effect of subgroup (First: $f^2 = 0.23$, p = 0.482; Last: $f^2 = 0.11$, p = 0.709). Importantly, effects are moderate and non-significant on the last night, when subgroup assignment may have theoretically had the greatest impact. Overall, these results indicate that changes in SWA during and after stimulation are similar across subgroups and supports the decision to pool their data. Further

ARTICLE IN PRESS

supporting this approach is that a main effect of period was found for both first and last nights (First: $f^2 = 0.90$, $p = 1.42x10^{-5}$; Last: $f^2 = 0.84$, $p = 2.66x10^{-6}$). Thus, the qualitative conclusions are the same–that SWA increases during and after TES^{15kHz}-TI^{1Hz} stimulation–whether the subgroups are factored in with the LME or whether the subgroups are aggregated.

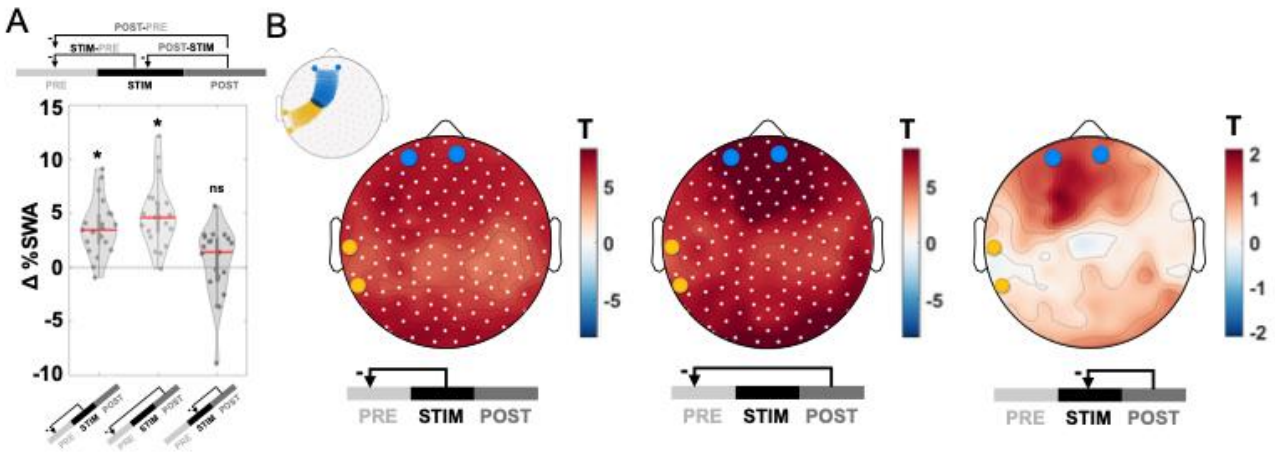

***Figure 3. TES^{15kHz}-TI^{1Hz} effects on SWA. A**. Across all channels, normalized SWA (%SWA) increases during and after TES^{15kHz}-TI^{1Hz} compared to before (N = 21; STIM-PRE, t = 6.64, $p = 4.97x10^{-6}$, d = 1.45; POST-PRE, t = 7.46, $p = 1.86x10^{-6}$, d = 1.63). %SWA does not change after stimulation compared to during stimulation (POST-STIM, t = 0.63, p = 0.982, d = 0.14). Two-sided paired samples t-tests, Benjamini-Yekutieli procedure to correct for multiple comparisons. Median shown as solid red line. **B**. Increases in %SWA during and after stimulation are global. No channels have statistically significant changes in %SWA after stimulation compared to during stimulation. Topography of T-statistic shown; channels with statistically significant changes are indicated by white dots. Approximate locations of stimulating electrodes are shown in blue (E_1) and yellow (E_2).*

TES^{15kHz}-TI^{1Hz} effects on SWA during stimulation.

We then performed a comparison of the effects on SWA of TES with amplitude modulation (TES^{15kHz}-TI^{1Hz}, 1 Hz difference) and without (TES^{15kHz}, 0 Hz difference) during stimulation (**Figure 4A**). To do so, we directly compared normalized SWA (%SWA) in the STIM period between TES^{15kHz}-TI^{1Hz} and TES^{15kHz}. Using nonparametric cluster-based statistics, we find a broad set of channels with SWA that is significantly greater in TES^{15kHz}-TI^{1Hz} as compared to TES^{15kHz} (**Figure 4B**, Left, 1 positive cluster, 116 significant electrodes, $\bar{p}$=0.028). In the average across these channels, SWA during TES^{15kHz}-TI^{1Hz} is greater than SWA during TES^{15kHz} (**Figure 4B**, Right, TES^{15kHz}-TI^{1Hz} N = 21, TES^{15kHz} N = 7, t = 2.47, p = 0.020, d = 1.08, two-sided independent samples t-test).

We also tested whether the effects on SWA changed throughout the STIM period during TES^{15kHz}-TI^{1Hz}. For this analysis, we compared the last 45 seconds (LATE) of the STIM period with the first 45 seconds (EARLY), including the 15-second ramping interval (**Figure 4C**). During TES^{15kHz}-TI^{1Hz}, SWA is higher in LATE compared to EARLY, and these increases in LATE SWA are global and strongest in the frontal region (**Figure 4C,** Left, 1 positive cluster, 168 significant electrodes, $\bar{p}=9.31x10^{-3}$**; Figure 4C**, Right, N=21, t=3.47, $p=2.41x10^{-3}$, d=0.76; two-sided paired samples t-test). Similar patterns suggesting increased SWA during TES^{15kHz}-TI^{1Hz} as compared to TES^{15kHz}, and during LATE TES^{15kHz}-TI^{1Hz} as compared to EARLY, are found when using a narrower frequency band surrounding SWA, 0.5-2 Hz (**Supplementary Figure 3B, C**).

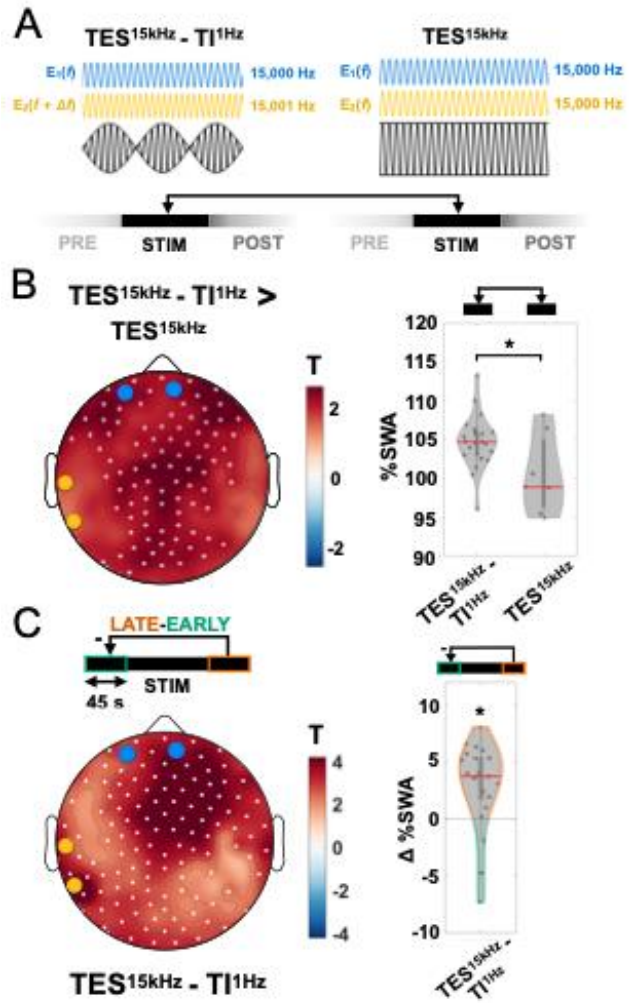

Figure 4. TES^{15kHz}-TI^{1Hz} effects on SWA during stimulation. ***A***. *In TES^{15kHz}-TI^{1Hz}, one pair of electrodes delivers high frequency alternating current with an offset (15,001 Hz) to create temporal interference (amplitude modulation) at 1 Hz. In TES^{15kHz}, both pairs of electrodes deliver the same high frequency alternating current, with no offset, i.e. there is no amplitude modulation (difference is 0 Hz). Normalized SWA (%SWA) during the stimulation period (STIM) is directly compared between TES^{15kHz}-TI^{1Hz} and TES^{15kHz}.* ***B***. *(Left) During stimulation, %SWA is increased across widespread channels in TES^{15kHz}-TI^{1Hz} as compared to TES^{15kHz}. (Right) Average %SWA across channels with statistically significant differences between TES^{15kHz}-TI^{1Hz} and TES^{15kHz} is shown. %SWA is higher during TES^{15kHz}-TI^{1Hz} as compared to TES^{15kHz} (TES^{15kHz}-TI^{1Hz} N = 21, TES^{15kHz} N = 7, t = 2.47, p = 0.020, d = 1.08, two-sided independent samples t-test). Median shown as solid red*

ARTICLE IN PRESS

*line. **C**. Within the three-minute period during stimulation, EARLY and LATE forty-five second intervals are considered; the difference in %SWA between the LATE and EARLY stimulation intervals are compared during TES^{15kHz}-TI^{1Hz}. (Left) %SWA is greater in the LATE interval compared to the EARLY interval during TES^{15kHz}-TI^{1Hz}. Increases in %SWA later in stimulation are global. (Right) Averaged across all channels with statistically significant increases, %SWA is greater in the LATE interval ($N = 21$, $t = 3.47$, $p = 2.41x10^{-3}$, $d = 0.76$, two-sided paired samples t-tests). Topography of T-statistic shown; channels with statistically significant changes are indicated by white dots. Approximate locations of stimulating electrodes are shown in blue (E_1) and yellow (E_2).*

TES^{15kHz}-TI^{1Hz} effects on other frequency bands.

Next, we tested whether TES^{15kHz}-TI^{1Hz} had additional effects on the EEG power spectrum. PSD values were averaged for each PRE, STIM, and POST period, then across electrodes, then across first and last intervention night, to yield one spectrum per participant (N=21). Spectra were then averaged across participants (**Figure 5**). For each frequency bin (N=240, 0.167 Hz steps), the STIM-PRE difference, as well as the POST-PRE difference, were calculated. For statistical comparisons, for each canonical band (e.g., theta, alpha), PSD values were averaged across the frequencies in that band for each participant, then STIM-PRE and POST-PRE comparisons were performed using paired samples t-tests with correction for multiple comparisons (**Supplementary Table 2**). For selected significant topographical analyses, as was done with SWA, band power was normalized (% band power) by the average band power during NREM throughout the entire night to give a relative change from the mean overnight band power. Then, the difference between time periods (STIM-PRE, POST-PRE) was evaluated with nonparametric cluster-based statistics.

We find that, as compared to before, during stimulation, TES^{15kHz}-TI^{1Hz} increases power in the theta (4–8 Hz) range and decreases power in the beta (16–25 Hz) range (**Figure 5A**, STIM-PRE, N = 21, theta: t = 4.28, p = 0.011, d = 0.93; beta: t = -3.30, p = 0.034, d = -0.72; two-sided paired samples t-tests). Both changes are global (**Figure 5B,** theta: 1 positive cluster, 185 significant electrodes, $\bar{p} = 8.97x10^{-4}$; beta: 1 negative cluster, 173 significant electrodes, $\bar{p} = 7.67x10^{-3}$). As compared to before stimulation, after TES^{15kHz}-TI^{1Hz}, we find an increase in power in the theta range and a decrease in the sigma (12–16 Hz) range (**Figure 5C**, POST-PRE, N = 21, theta: t = 3.90, $p = 8.92x10^{-4}$, d = 0.85; sigma: t = -3.95, $p = 7.95x10^{-4}$, d = -0.86; two-tailed paired samples t-tests). All these changes are also global (**Figure 5D**, theta: 1 positive cluster, 185 significant electrodes, $\bar{p} = 1.35x10^{-3}$; sigma: 1 negative cluster, 185 significant electrodes, $\bar{p} = 4.44x10^{-3}$). Analyses were also repeated for the TES^{15kHz} group, but given the small samples size, results should be considered exploratory and hypothesis-generating (**Supplementary Table 3**).

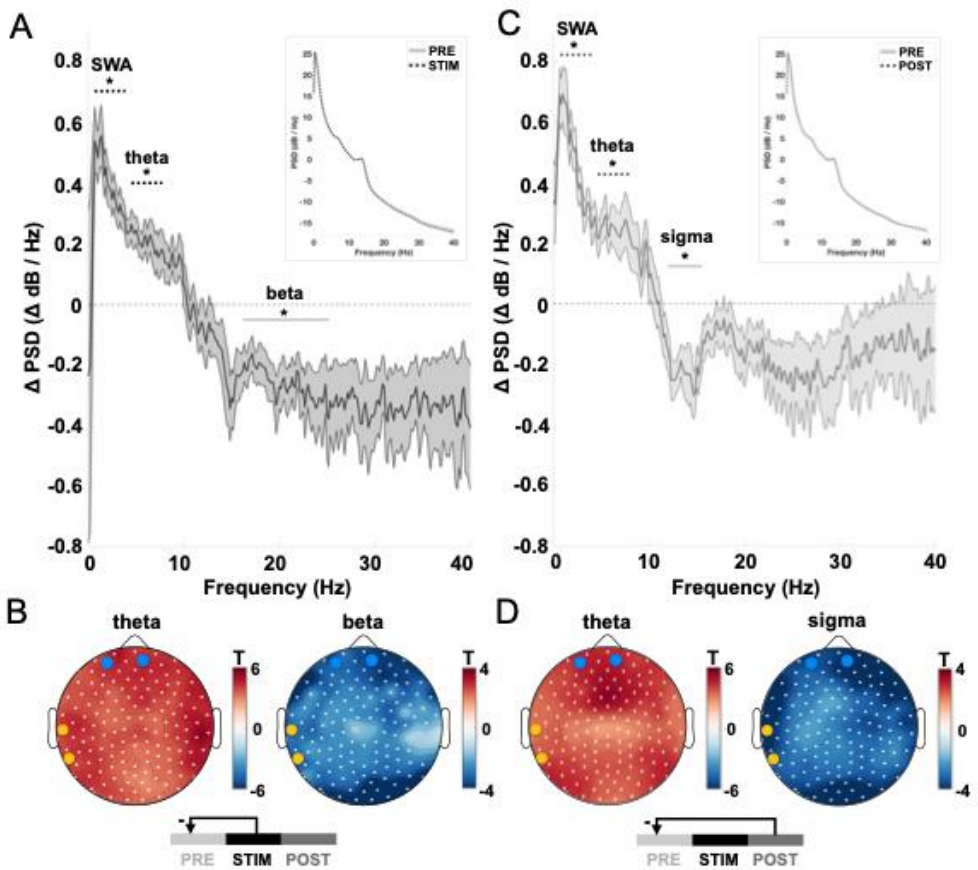

Figure 5. TES^{15kHz}-TI^{1Hz} effects on other frequency bands. ***A****. Differences in power spectral density (PSD) during (STIM) compared to before (PRE) stimulation for individual frequencies (N=240, 0.167 Hz steps). PSD is averaged across channels then across participants (dark line) with the standard error of the mean across participants (light lines) shown. In addition to SWA (Figure 2), increased theta and decreased beta power are found during stimulation (N = 21; theta: t = 4.28, p = 0.011, d = 0.93; beta: t = -3.30, p = 0.034, d = -0.72). Two-sided paired samples t-tests, Benjamini-Yekutieli procedure to correct for multiple comparisons. (Top Right, Inset) PSD for individual frequencies before (PRE) and during (STIM) stimulation.* ***B****. Changes in normalized theta and normalized beta power are global.* ***C****. Differences in PSD after (POST) compared to before (PRE) stimulation. In addition to SWA (Figure 2), increased theta and decreased sigma power are found after stimulation (N = 21; theta: t = 3.89, p = 0.011, d = 0.85; sigma: t = -3.95, p = 0.011, d = -0.86). Two-sided paired samples t-tests, Benjamini-Yekutieli procedure to correct for multiple comparisons. (Top Right, Inset) PSD for individual frequencies before (PRE) and after (POST) stimulation.* ***D****. Changes in normalized theta and normalized sigma power are global. Topography of T-statistic shown; channels with statistically significant changes are indicated by white dots. Approximate locations of stimulating electrodes are shown in blue (E_1) and yellow (E_2).*

Changes in SWA during TES^{15kHz}-TI^{1Hz} are associated with improved sleep quality ratings following the TES^{15kHz}-TI^{1Hz} intervention.

Finally, we examined potential relationships between stimulation-related changes in normalized SWA (%SWA) and participants' perceptions of how they slept. For each participant in the TES^{15kHz}-TI^{1Hz} group, we compared the difference in SWA during (STIM-PRE) and after (POST-PRE) TES^{15kHz}-TI^{1Hz} with subjective sleep quality ratings from the Restorative Sleep Questionnaire (REST-Q) [44,45], assessed the

morning after each intervention night. In line with Robbins and colleagues [44], an overall REST-Q score was calculated for each participant and each intervention night.

To identify potential factors associated with overall REST-Q scores, we used a predictive modeling approach, specifically Least Absolute Shrinkage and Selection Operator (LASSO) estimation with 5-fold cross-validation. Power across all channels in SWA, theta, beta, low sigma, and high sigma bands during STIM-PRE and POST-PRE periods (independent variables) were used as predictors for overall REST-Q ratings (dependent variable). The model was fit on first and last night data as well as the difference between last and first nights to assess for longitudinal changes over the course of the intervention in the context of inter-individual variability.

For first and last night data ($\lambda\_min = 2.98$, cross-validated Mean Squared Error (MSE) = 313.0), no factors improve predictive performance. For the difference between last and first nights ($\lambda\_min = 9.44$, cross-validated MSE = 298.6), only one factor improves predictive performance: the change in SWA during the STIM-PRE period. Specifically, this factor has a positive regression coefficient, indicating that greater increases in SWA during TES^{15kHz}-TI^{1Hz} (STIM-PRE) on the last night compared to the first night are associated with higher overall REST-Q scores on the last night compared to the first night. To visualize the predictive model, we fit a simple linear regression model and extracted the line of best fit and R^2 values (**Figure 6A**, Left, $\beta_1 = 2.20$, $R^2 = 0.38$). To further investigate whether the predictive power in the observed data was spatially localized, R^2 values are plotted topographically (**Figure 6A**, Right). We find relatively high R^2 values globally, with the greatest values in the left frontal region. However, we note that these topographies are purely descriptive. Changes in sigma power (STIM-PRE) are shown as an example of a factor that does not improve predictive performance of the model (**Figure 6B**, high sigma: 12–16 Hz, N = 16, $\beta_1 = -0.43$, $R^2 = 0.05$).

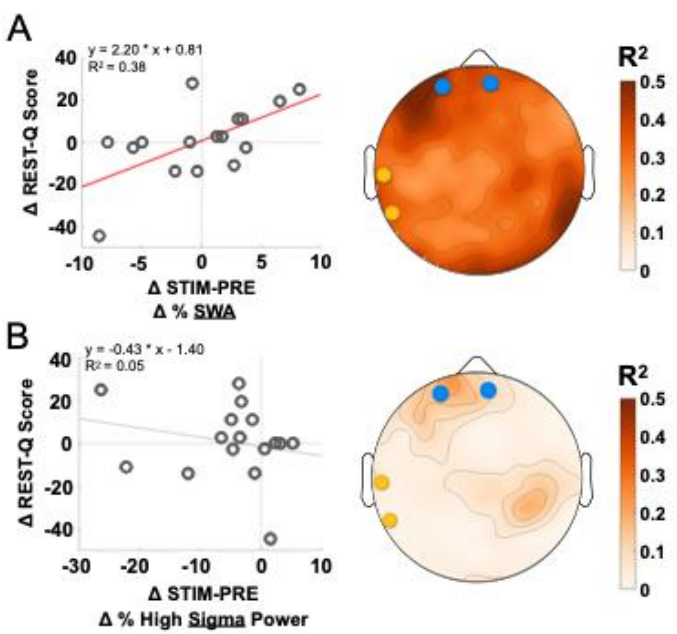

Figure 6. Relationship between changes in SWA during TES^{15kHz}-TI^{1Hz} and changes in sleep quality following TES^{15kHz}-TI^{1Hz} intervention. *Greater increases in normalized SWA (%SWA), averaged across all channels, are related to improved sleep quality in TES^{15kHz}-TI^{1Hz}. **A**. (Left) Difference in %SWA during stimulation (STIM-PRE, x-axis) is positively associated with the difference in overall REST-Q scores on the last intervention night as compared to the first intervention night (y-axis) ($N = 16$, $\beta_1 = 2.20$, $R^2 = 0.38$). (Right) Strongest relationships are present in left frontal areas. Topography of R^2 values is shown.* ***B.*** *(Left) Difference in*

ARTICLE IN PRESS

normalized 12–16 Hz (high sigma) power during stimulation (STIM-PRE, x-axis) was not associated with the difference in overall REST-Q scores on the last intervention night as compared to the first intervention night (y-axis) (N = 16, β_1 = -0.43, R^2 = 0.05). (Right) On topography, most areas had R^2 values near zero. Approximate locations of stimulating electrodes are shown in blue (E_1) and yellow (E_2).

Discussion

We performed simultaneous hd-EEG recording and Transcranial Electrical Stimulation with Temporal Interference (TES-TI, 15 kHz, 1 Hz difference) during overnight sleep in a laboratory setting in healthy humans with the goal of enhancing SWA during NREM sleep. Baseline, first, and last nights over the course of the 4-week STRENGTHEN study protocol were included in this interim report. The results show that TES^{15kHz}-TI^{1Hz} targeting left ventromedial prefrontal cortical regions increased SWA during the stimulation period, and the effect outlasted the stimulation. TES^{15kHz}-TI^{1Hz} during the stimulation period also increased SWA compared to TES^{15kHz} without TI (15 kHz, 0 Hz difference), suggesting that the effect may be specifically attributable to TI. During TES^{15kHz}-TI^{1Hz} stimulation, increases in SWA were greater in the late part of the stimulation interval. Effects on spectral power in other frequency bands were also found, pointing to an overall increase in low frequencies (SWA and theta range) and a decrease in higher frequencies (sigma and beta range) during and/or after stimulation. Lastly, participants who showed the largest incremental effects on SWA between the first and the last intervention night of the 4-week protocol also showed the largest improvement in restorative sleep ratings. Together, these findings support the ability of TES^{15kHz}-TI^{1Hz} to enhance SWA and, more generally, the potential for TES-TI as an intervention to improve sleep.

TES-TI offers several potential advantages compared to other techniques for neuromodulation during sleep. While acoustic stimulation increases SWA [13,19,20,64], the closed-loop titration of the intensity of stimuli to effectively trigger slow waves without awakening subjects can be problematic. This is likely because the triggering of slow waves is mediated by the non-lemniscal auditory pathway, which is associated with the ascending reticular activating system (ARAS) in the brainstem [13]. By directly modulating slow wave generation within their primary cortical origination sites, TES-TI circumvents unintended ARAS activation. Indeed, when comparing general sleep architecture metrics, which were comparable to [65], across baseline, first and last intervention nights, we found that TES^{15kHz}-TI^{1Hz} did not affect the sleep architecture and, more specifically, did not increase the number of arousals, arousal index, number of awakenings, or the time spent awake after sleep onset. Notably, the percent of time spent in slow wave sleep (Stage N3) and SWA (both throughout the entire night and in the first four hours of sleep) did not change across baseline, first, and last intervention nights for TES^{15kHz}-TI^{1Hz} participants. This is in line with several studies using an ON/OFF block design to enhance SWA with other methods [18]. It is possible that more numerous stimulation protocols and/or continuous stimulation might expand the increases in SWA observed in the immediate 3-minutes during and after TES^{15kHz}-TI^{1Hz} to a larger timescale, over several hours. Also consistent with the preservation of sleep architecture was that the power spectra before, during, and after stimulation all maintained a profile consistent with NREM sleep, including a large, broad peak in the low frequencies corresponding to SWA and a smaller peak in the higher frequencies corresponding to sigma power.

Conventional TES, which typically employs frequencies below 1 kHz, has also been used to increase sleep SWA [15,19,66,67]. However, conventional TES is not well suited for reaching deep brain regions and to do so focally, it produces scalp discomfort and potential awakenings at relatively low stimulation intensities (e.g., 1.5 mA). Also, electrical artifacts prevent the analysis of concurrent EEG recordings [18]. By contrast, TES^{15kHz}-TI^{1Hz} as performed in this study, can reach deep brain regions with relatively high focality

ARTICLE IN PRESS

and field intensity, as indicated by electric field modeling of the interference field for individual subjects. Even at the relatively high intensities employed in this study (5 mA), TES^{15kHz}-TI^{1Hz} did not produce any scalp sensation and did not awaken subjects. In addition, given the high carrier frequency (15 kHz, much higher than the EEG signal) and the use of dedicated hardware filters, it was possible to conduct simultaneous TES^{15kHz}-TI^{1Hz} and hd-EEG recordings avoiding stimulation artifacts (there were no narrow peaks at 1Hz or its harmonics superimposed on the smooth power spectra typical of NREM sleep).

TES^{15kHz}-TI^{1Hz} was intentionally targeted to a deep brain region—left ventromedial prefrontal cortical regions that we had previously identified as a "hot spot" for the origination of slow waves through source modeling of all-night hd-EEG recordings [40]. Because slow waves travel across the cortical surface [68] we nevertheless suspected that the effects of targeted neuromodulation might extend to broader cortical areas. In fact, the increases in SWA during and after TES^{15kHz}-TI^{1Hz} were global, extending across all channels.

An interesting aspect of the present results is that the increase in SWA produced by TES^{15kHz}-TI^{1Hz} was incremental—increasing from the beginning to the end of the 3-minute stimulation period, as SWA was higher in the last 45-seconds of stimulation compared to the first. Increases in SWA also outlasted the stimulation, extending to the subsequent 3 minutes. These findings suggest that TES^{15kHz}-TI^{1Hz} at 1 Hz may not simply boost, synchronize, or entrain neuronal slow oscillations, but may produce plastic changes that underlie a cumulative effect. The extent of these changes may be more formally assessed by future studies that systematically vary the duration of the stimulation period. Overall, these findings clearly warrant further investigation of stimulation protocols that may maximize the effectiveness of SWA enhancement by lengthening stimulation periods, increasing the number of stimulation periods, and/or repeating them over subsequent nights.

An important part of this study was the direct comparison of TES^{15kHz}-TI^{1Hz} and TES^{15kHz}. A separate group of participants (N = 7) received high frequency stimulation (15 kHz) with the same intensity and duration as the TES^{15kHz}-TI^{1Hz} group, but with 0 Hz frequency difference between the two stimulation channels (TES^{15kHz}). High frequency TES is often assumed to produce minimal effects on the brain because of dampening of the field intensity by the skull, resulting in subthreshold intensities, but this assumption has not yet been tested fully [39,69]. The present results showed that TES^{15kHz}-TI^{1Hz}, compared to TES^{15kHz}, increased SWA during the stimulation period. This initial finding supports the notion that the focal amplitude modulation at 1 Hz obtained through TES^{15kHz}-TI^{1Hz} has specific effects on brain activity that are not observed by mere high frequency TES^{15kHz}, consistent with data from intracranial recordings [39].

Besides increasing sleep SWA, the TES^{15kHz}-TI^{1Hz} intervention employed here produced changes in the sleep power spectrum that were consistent with an overall deepening of sleep. In addition to increased power in the SWA (delta) band, we observed a global increase in theta power during and after TES^{15kHz}-TI^{1Hz} stimulation. Sleep onset is typically accompanied by an increase in both delta and theta power [70,71] and recovery sleep is characterized by increases in low frequency power that extend into the theta band [72-75]. An increase in theta activity continuous with an increase in SWA is an expected consequence of increased sleep pressure [2,3,72-75]. Similarly, the global decrease in beta power concomitant with increased SWA during TES^{15kHz}-TI^{1Hz} was consistent with the inverse relationship between beta and delta power and the higher delta:beta ratio associated with reduced arousal levels [71,76]. The decrease in power in the sigma range (12–16 Hz) after TES^{15kHz}-TI^{1Hz} (and a trend during TES^{15kHz}-TI^{1Hz}) may also reflect a deepening of sleep. In general, a reduction in spindles is seen with the transition to slow wave sleep (Stage N3), in recovery sleep after total sleep deprivation [72,75] and, in particular, fast spindle power has dynamics that run in the opposite direction of those of SWA [77-79]. In addition, as supported by intracranial EEG in humans,

ARTICLE IN PRESS

maximal SWA accompanied by decreases in spindle density and frequency are most evident in earlier NREM sleep, consistent with when most stimulation protocols were performed in this study [80,81].

A promising, albeit preliminary, indication of this study was the improvement in the restorative quality of sleep when comparing the first and last intervention nights of TES^{15kHz}-TI^{1Hz}, as reported by subjects through REST-Q scores. Specifically, participants with greater increases in SWA during TES^{15kHz}-TI^{1Hz} from the first to the last night also reported better overall restorative sleep ratings. This relationship was specific to sleep SWA, as it did not extend to the other frequency bands tested (theta, beta, sigma). The ability of TES^{15kHz}-TI^{1Hz} to produce effects on neuronal activity during sleep that outlast the stimulation and may be associated with plastic changes, as identified here, will be further investigated in the STRENGTHEN study by assessing long-lasting modifications in brain anatomical and functional connectivity, as well as in behavioral indicators of cognitive flexibility and emotional regulation [82,83].

This study of TES-TI during sleep had several limitations. We targeted left ventromedial prefrontal cortex using a standardized montage for TES^{15kHz}-TI^{1Hz}. Future work may determine whether more precise, individualized TES-TI targeting may offer superior efficacy [51,84]. Our initial analyses focused on the effects of TES^{15kHz}-TI^{1Hz} during NREM sleep on first and last intervention nights. Future work within the STRENGHTEN framework will evaluate additional intervention nights as well as the effects of TES^{15kHz}-TI^{6Hz} during REM sleep. Further enrollment will increase the number of subjects receiving TES^{15kHz} and possibly add a within-participant component. On the other hand, few clinical trials of TES-TI have provided a direct comparison with TES [39], as was done here.

SWA varies with age, and the age range in this study is relatively wide (19–49 years). However, we assessed the effect of TES^{15kHz}-TI^{1Hz} with an intra-subject design, by comparing adjacent 3-minute periods and normalizing power to the entire night [59,71,85,86]. While fluctuations of SWA during NREM episodes can present a challenge, the use of multiple stimulation blocks (repeated ten times per night) primarily throughout the first four hours of NREM sleep was intended to avoid spurious effects associated with infra-slow oscillations or the natural deepening of sleep. Future studies will aim at identifying the optimal parameters for TES-TI stimulation, including duration and timing, informed by increasing knowledge about its mechanism of action [22,26,29,30]. Moreover, the ability of TES-TI to modulate other features of sleep, from sleep spindles to sawtooth waves to sharp-wave ripples, are also ready for exploration, with potential applications in health and disease.

Conclusions: To our knowledge, this interim analysis of data from the STRENGTHEN study provides the first evidence in support of the ability of TES-TI (15 kHz, 1 Hz difference) targeting left ventromedial prefrontal cortex to increase SWA during and after stimulation. Participants with the greatest longitudinal increases in SWA during TES-TI also have the greatest improvements in ratings of restorative sleep, potentially indicating beneficial effects of TES-TI on sleep.

ARTICLE IN PRESS

Data Availability

Data needed to reproduce tables and figures for the main results are provided as Supplementary Data files. Specifically:

Source data for Tables 1–3 are in Supplementary Data 1.
Source data for Figure 3 are in Supplementary Data 2.
Source data for Figure 4 are in Supplementary Data 3.
Source data for Figure 5 are in Supplementary Data 4.
Source data for Figure 6 are in Supplementary Data 5.

All source data for Figures 3–6, Tables, and Supplementary Tables and Figures are also publicly available via generalist repository (https://doi.org/10.5281/zenodo.18653921) ref. [87].
Access to the unprocessed data underlying this article is available upon reasonable request to the corresponding authors.

Code Availability

Customized codes used to create the main figures and tables have been made publicly available via generalist repository (https://doi.org/10.5281/zenodo.18653921) ref. [87].

ARTICLE IN PRESS

Acknowledgements

We thank Tricia Denman, Emily Peterson, and Kate Riordan for their efforts in participant recruitment, Everett Carstens, Claire Doucet, Paul Ladefoged, Poorang Nori, and Ana Maria Vascan for their efforts in data collection, Cameron Brace and Dillon Scott for their assistance in data processing.
This project is funded by the Defense Advanced Research Projects Agency (DARPA) under cooperative agreement No. HR00112320033 (to G.T., R.J.D.). The content of the information does not necessarily reflect the position or the policy of the Government, and no official endorsement should be inferred.
The TIBS-R investigational devices used in this project were provided by TI Solutions AG, Switzerland, as part of its Early Adopter Program (www.temporalinterference.com).
This work was also supported by the following: the JSPS Fund for the Promotion of Joint International Research, Grant Number 22K21351 (to Z.F.), the Ministry of Health of the Czech Republic in cooperation with the Czech Health Research Council in the context of the RECOVERY project under No. NW25J-04-00094 (to F.M.), and the European Union's Horizon Europe research and innovation program under grant agreement No. 101157945 (FITSLEEP, to A.W.).

Author Contributions

Conceptualization – G.T., R.J.D., S.G.J., R.I.G., C.C., M.B., E.L.S., I.H.; Data Curation – E.L.S., I.H., Z.F., S.Br., B.M., R.S., S.G.J., L.A., M.B.; Formal Analysis – E.L.S., W.M., S.Br., I.H., Z.F., L.N.; Funding Acquisition – G.T., R.J.D., S.G.J., R.I.G.; Investigation – E.L.S., I.H., B.M., T.A., G.V., R.S., L.N.; Methodology – G.T., S.G.J., M.B., E.L.S., I.H., Z.F., S.Br., W.M., L.A., F.M., A.W., P.A., S.Be., M.C., E.N., N.K.; Project Administration – S.G.J., E.L.S., B.M., R.S., M.B.; Resources – P.A., S.Be., M.C., E.N., N.K.; Software – E.L.S., W.M., I.H., Z.F., S.Br., P.A., S.Be., M.C., E.N., N.K.; Visualization – E.L.S., S.Br., W.M., I.H., Z.F.; Writing (Original Draft) – E.L.S., C.C., G.T.; Writing (Review & Editing) – all authors.

Competing Interests

ARTICLE IN PRESS

The authors declare no competing financial or non-financial interests, with the following exceptions: G.T. is Chair of Board and has a financial interest in Intrinsic Powers Inc., N.K. and E.N. are Board Members and have a financial interest in TI Solutions AG, and R.J.D. is the founder, president, and serves on the board of directors for the nonprofit organization, Healthy Minds Innovations, Inc.

ARTICLE IN PRESS

ARTICLE IN PRESS

References

1. Steriade, M., *et al*. Natural waking and sleep states: a view from inside neocortical neurons. *Journal of neurophysiology* **85**, 1969-1985 (2001).
2. Borbély, A.A. A two process model of sleep regulation. *Human Neurobiol.* **1**, 195-204 (1982).
3. Borbely, A.A., *et al*. The two-process model of sleep regulation: a reappraisal. *J Sleep Res* **25**, 131-143 (2016).
4. Franken, P. & Dijk, D.J. Sleep and circadian rhythmicity as entangled processes serving homeostasis. *Nat Rev Neurosci* **25**, 43-59 (2024).
5. Gulati, T., *et al*. Neural reactivations during sleep determine network credit assignment. *Nature neuroscience* **20**, 1277-1284 (2017).
6. Liu, J., *et al.* Slow-wave sleep drives sleep-dependent renormalization of synaptic AMPA receptor levels in the hypothalamus. *PLoS Biol* **22**, e3002768 (2024).
7. Squarcio, F., *et al*. Effects of non-rapid eye movement sleep on the cortical synaptic expression of GluA1-containing AMPA receptors. *The European journal of neuroscience* **60**, 3961-3972 (2024).
8. Tononi, G. & Cirelli, C. Sleep and the price of plasticity: from synaptic and cellular homeostasis to memory consolidation and integration. *Neuron* **81**, 12-34 (2014).
9. Diekelmann, S., & Born, J. The memory function of sleep. *Nature reviews* **11**, 114-126 (2010).
10. Born, J. Slow-wave sleep and the consolidation of long-term memory. *World J. Biol. Psychiatry* **11**, 16-21 (2010).
11. Brodt, S., *et al*. Sleep-A brain-state serving systems memory consolidation. *Neuron* **111**, 1050-1075 (2023).
12. Landsness, E.C., *et al.* Sleep-dependent improvement in visuomotor learning: a casual role for slow waves. *Sleep* **32**, 1273-1284 (2009).
13. Bellesi, M., *et al*. Enhancement of sleep slow waves: underlying mechanisms and practical consequences. *Front Syst Neurosci* **8**, 208 (2014).
14. Aeschbach, D., *et al*. A role for non-rapid-eye-movement sleep homeostasis in perceptual learning. *J. Neurosci* **28**, 2766-2772 (2008).
15. Marshall, L., *et al*. Transcranial direct current stimulation during sleep improves declarative memory. *J. Neurosci* **24**, 9985-9992 (2004).
16. Wunderlin, M., *et al.* Acoustic stimulation during sleep predicts long-lasting increases in memory performance and beneficial amyloid response in older adults. *Age Ageing* **52**, afad228 (2023).
17. Diep, C., *et al.* Acoustic slow wave sleep enhancement via a novel, automated device improves executive function in middle-aged men. *Sleep* **43**, zsz197 (2020).
18. Feher, K.D., *et al.* Shaping the slow waves of sleep: A systematic and integrative review of sleep slow wave modulation in humans using non-invasive brain stimulation. *Sleep Med Rev* **58**, 101438 (2021).
19. Krugliakova, E., *et al*. Hacking the functions of sleep: noninvasive approaches to stimulate sleep neurophysiology. *Physiological reviews*, **106**, 675–749 (2026).
20. Tononi, G., *et al*. Enhancing sleep slow waves with natural stimuli. *Medicamundi* **54**, 73-79 (2010).
21. Louviot, S., *et al.* Transcranial electrical stimulation generates electric fields in deep human brain structures. *Brain stimulation* **15**, 1-12 (2022).
22. Grossman, N., *et al.* Noninvasive deep brain stimulation via temporally interfering electric fields. *Cell* **169**, 1029-1041 e1016 (2017).

ARTICLE IN PRESS

23. Ganne, J. M. Interferential therapy. *Aust. J. Physiother* **22**, 101-110 (1976).
24. Goats, G.C. Interferential current therapy. *Br. J. Sports Med* **24**, 87-92 (1990).
25. Ward, A.R. Electrical stimulation using kilohertz-frequency alternating current. *Phys. Ther* **89**, 181-190 (2009).
26. Opancar, A., *et al*. The same biophysical mechanism is involved in both temporal interference and direct kHz stimulation of peripheral nerves. *Nature Communications* **16**, 9006 (2025).
27. Thiele, C., *et al*. Perceptibility and Pain Thresholds in Low- and High-Frequency Alternating Current Stimulation: Implications for tACS and tTIS. *Journal of Cognitive Enhancement* (2024).
28. Vassiliadis, P., *et al*. Safety, tolerability and blinding efficiency of non-invasive deep transcranial temporal interference stimulation: first experience from more than 250 sessions. *J Neural Eng* **21**(2024).
29. Mirzakhalili, E., *et al*. Biophysics of temporal interference stimulation. *Cell Syst* **11**, 557-572 (2020).
30. Caldas-Martinez, S., *et al*. Cell-specific effects of temporal interference stimulation on cortical function. *Communications biology* **7** 1076 (2024).
31. Piao, Y., *et al*. Safety Evaluation of Employing Temporal Interference Transcranial Alternating Current Stimulation in Human Studies. *Brain sciences* **12**, 1194 (2022).
32. Wang, Y., *et al*. The safety and efficacy of applying a high-current temporal interference electrical stimulation in humans. *Front Hum Neurosci* **18**, 1484593 (2024).
33. Violante, I.R., *et al*. Non-invasive temporal interference electrical stimulation of the human hippocampus. *Nature neuroscience* **26**, 1994-2004 (2023).
34. Mansourinezhad, P., *et al.* Systematic review of experimental studies in humans on transcranial temporal interference stimulation. *J Neural Eng* **22**, (2025).
35. Albantakis L. & Tononi G. Precision neuromodulation in psychiatry: focus on temporal interference stimulation. (in press at *Am. J. of Psychiatry*) (2026).
36. Kurtin, D. L., *et al*. Task-related changes in resting state connectivity are affected by temporal interference (TI) stimulation. *Brain stimulation* **18,** 937–947 (2025).
37. Beanato, E., *et al*. Noninvasive modulation of the hippocampal-entorhinal complex during spatial navigation in humans. *Sci Adv* **10**, eado4103 (2024).
38. Thiele, C., *et al*. Transcranial temporal interference stimulation (tTIS) influences event-related alpha activity during mental rotation. *Psychophysiology* **61**, e14651 (2024).
39. Missey, F., *et al*. Non-invasive temporal interference stimulation of the hippocampus suppresses epileptic biomarkers in patients with Epilepsy: biophysical differences between kilohertz and amplitude modulated stimulation. *Brain stimulation* **19,** 102981 (2026).
40. Murphy, M.J., *et al.* Source modeling sleep slow waves. *Proceedings of the National Academy of Sciences of the United States of America* **106**, 1608-1613 (2009).
41. Nir, Y., *et al.* Regional slow waves and spindles in human sleep. *Neuron* **70**, 153-169 (2011).
42. Davidson, R. J. Mindfulness and more: toward a science of human flourishing. *Psychosom Med* **83**, 665-668 (2021).
43. Hirshberg M., *et al*. A randomized controlled trial of a smartphone-based well-being training in public school system employees during the COVID-19 pandemic. *J Educ Psychol*. **114**, 1895-1911 (2022).
44. Robbins, R., *et al.* A Nationally Representative Survey Assessing Restorative Sleep in US Adults. *Front Sleep* **1**, 935228 (2022).
45. Drake, C.L., *et al*. Development and evaluation of a measure to assess restorative sleep. *J Clin Sleep Med* **10**, 733-741, 741A-741E (2014).

ARTICLE IN PRESS

46. Cassara, A.M., *et al.* Recommendations for the safe application of temporal interference stimulation in the human brain part I: principles of electrical neuromodulation and adverse effects. *Bioelectromagnetics* **46**, e22542 (2025).
47. Cassara, A.M., *et al.* Recommendations for the safe application of temporal interference stimulation in the human brain part II: biophysics, dosimetry, and safety recommendations. *Bioelectromagnetics* **46**, e22536 (2025).
48. Iacono, M.I., *et al.* MIDA: A Multimodal Imaging-Based Detailed Anatomical Model of the human head and neck. *PloS one* **10**, e0124126 (2015).
49. Windhoff, M., *et al*. Electric field calculations in brain stimulation based on finite elements: an optimized processing pipeline for the generation and usage of accurate individual head models. *Hum Brain Mapp* **34**, 923-935 (2013).
50. Saturnino, G.B., *et al*. Optimizing the electric field strength in multiple targets for multichannel transcranial electric stimulation. *J Neural Eng* **18**, 10.1088 (2021).
51. Haber, I., *et al*. TI-Toolbox: An open-source software for temporal interference stimulation research. *Brain stimulation*, **19**, 103016 (2026).
52. Cox, R.W. AFNI: software for analysis and visualization of functional magnetic resonance neuroimages. *Computers and biomedical research, an international journal* **29**, 162-173 (1996).
53. Cox, R.W. & Hyde, J.S. Software tools for analysis and visualization of fMRI data. *NMR Biomed* **10**, 171-178 (1997).
54. Berry, R.B., *et al.* The AASM Manual for the Scoring of Sleep and Associated Events. Rules, terminology and technical specifications. Version 2.5. *American Academy of Sleep Medicine, Darien, IL*.
55. Delorme, A. & Makeig, S. EEGLAB: an open source toolbox for analysis of single-trial EEG dynamics including independent component analysis. *J Neurosci Methods* **134**, 9-21. (2004).
56. Jones, S.G., *et al.* Regional reductions in sleep electroencephalography power in obstructive sleep apnea: a high-density EEG study. *Sleep* **37**, 399-407 (2014).
57. Riedner, B.A., *et al*. Regional patterns of elevated alpha and high-frequency electroencephalographic activity during nonrapid eye movement sleep in chronic insomnia: a pilot study. *Sleep* **39**, 801-812 (2016).
58. Valomon, A., *et al.* A high-density electroencephalography study reveals abnormal sleep homeostasis in patients with rapid eye movement sleep behavior disorder. *Sci Rep* **11**, 4758 (2021).
59. Krugliakova, E., *et al.* Boosting recovery during sleep by means of auditory stimulation. *Front Neurosci* **16**, 755958 (2022).
60. Fattinger, S., *et al.* Deep sleep maintains learning efficiency of the human brain. *Nature communications* **8**, 15405 (2017).
61. Huber, R., *et al*. Local sleep and learning. *Nature* **430**, 78-81 (2004).
62. Nichols, T.E. & Holmes, A.P. Nonparametric permutation tests for functional neuroimaging: a primer with examples. *Hum Brain Mapp* **15**, 1-25 (2002)
63. Findlay, G., *et al*. A hippocampal 'sharp-wave sleep' state that is dissociable from cortical sleep. *Nature neuroscience* **29,** 399-410 (2026).
64. Riedner, B.A., *et al*. Temporal dynamics of cortical sources underlying spontaneous and peripherally evoked slow waves. *Progress in brain research* **193**, 201-218 (2011).
65. Stephan, A. M., *et al*. Conscious experiences and high-density EEG patterns predicting subjective sleep depth. *Current biology* **31**, 5487–5500 (2021).
66. Ketz, N., *et al*. Closed-loop slow-wave tACS improves sleep-dependent long-term memory generalization by modulating endogenous oscillations. *J. Neurosci* **38**, 7314-7326 (2018).

ARTICLE IN PRESS

67. Ladenbauer, J., *et al.* Promoting sleep oscillations and their functional coupling by transcranial stimulation enhances memory consolidation in mild cognitive impairment. *J. Neurosci* **37**, 7111-7124 (2017).
68. Siclari, F., *et al.* Two distinct synchronization processes in the transition to sleep: a high-density electroencephalographic study. *Sleep* **37**, 1621-1637 (2014).
69. Peterchev, A.V. One's trash is another's treasure: Subthreshold kilohertz brain modulation as a side effect and as an intervention. *Brain stimulation* **18**, 622-623 (2025).
70. Marzano, C., *et al.* How we fall asleep: regional and temporal differences in electroencephalographic synchronization at sleep onset. *Sleep medicine* **14**, 1112-1122 (2013).
71. Gorgoni, M., *et al.* The regional EEG pattern of the sleep onset process in older adults. *Brain sciences* **11**, 1261 (2021).
72. Borbely, A.A., *et al*. Sleep deprivation: effect on sleep stages and EEG power density in man. *Electroencephalogr Clin Neurophysiol* **51**, 483-495 (1981).
73. Aeschbach, D., *et al*. Dynamics of the human EEG during prolonged wakefulness: evidence for frequency-specific circadian and homeostatic influences. *Neuroscience letters*, **239**, 121–124 (1997).
74. Finelli, L. A., *et al*. Dual electroencephalogram markers of human sleep homeostasis: correlation between theta activity in waking and slow-wave activity in sleep. *Neuroscience*, **101**, 523–529 (2000).
75. Cajochen, C., *et al*. Frontal predominance of a relative increase in sleep delta and theta EEG activity after sleep loss in humans. *Sleep research online : SRO* **2**, 65–69 (1999).
76. Maes, J., *et al.* Sleep misperception, EEG characteristics and autonomic nervous system activity in primary insomnia: a retrospective study on polysomnographic data. *Int J Psychophysiol* **91**, 163-171 (2014).
77. Fernandez, L.M.J. & Luthi, A. Sleep spindles: mechanisms and functions. *Physiol Rev* **100**, 805-868 (2020).
78. Dijk, D.J. EEG slow waves and sleep spindles: windows on the sleeping brain. *Behav Brain Res* **69**, 109-116 (1995).
79. Uchida, S., *et al.* Sigma (12-15 Hz) and delta (0.3-3 Hz) EEG oscillate reciprocally within NREM sleep. *Brain research bulletin* **27,** 93–96 (1991).
80. Andrillon, T., *et al*. Sleep spindles in humans: insights from intrancranial EEG and unit recordings. *J. Neurosci.* **31**, 17821-17834 (2011).
81. Sarasso, S., *et al*. Thalamic and neocortical differences in the relationship between the time course of delta and sigma power during NREM sleep in humans. *Journal of sleep research* **30**, e13166 (2021).
82. Kesebir, P., *et al*. Emotional style questionnaire: a multidimensional measure of healthy emotionality. *Psychol Assess* **31**, 1234-1246 (2019).
83. Martin, M.M. & Rubin, R.B. A new measure of cognitive flexibility. *Psych Reports* **76**, 623-626 (1995).
84. Brahma, T., *et al*. On the need of individually optimizing temporal interference stimulation of human brains due to inter-individual variability. *Brain stimulation* **18**, 1373–1388 (2025).
85. Carrier, J., *et al.* Sleep slow wave changes during the middle years of life. *The European journal of neuroscience* **33**, 758-766 (2011).
86. Mander, B.A., Winer, J.R. & Walker, M.P. Sleep and human aging. *Neuron* **94**, 19-36 (2017).
87. Schaeffer, E. https://github.com/eschaeffer-0/Schaeffer_et_al_2026_comm_med. https://doi.org/10.5281/zenodo.18653921. (2026).